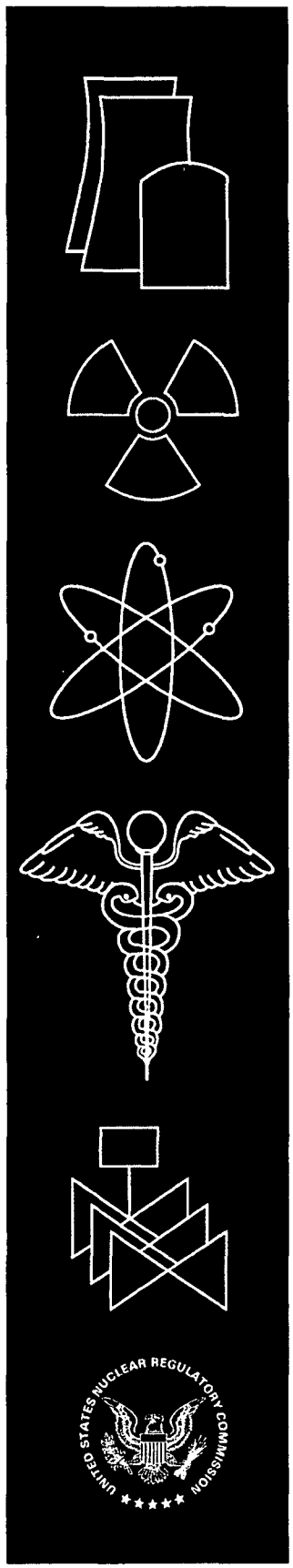

NUREG/CR-6935
ANL-04/04

Sensitivity Studies of Failure of Steam Generator Tubes during Main Steam Line Break and Other Secondary Side Depressurization Events

Argonne National Laboratory

U.S. Nuclear Regulatory Commission
Office of Nuclear Regulatory Research
Washington, DC 20555-0001

AVAILABILITY OF REFERENCE MATERIALS IN NRC PUBLICATIONS

NRC Reference Material

As of November 1999, you may electronically access NUREG-series publications and other NRC records at NRC's Public Electronic Reading Room at http://www.nrc.gov/reading-rm.html. Publicly released records include, to name a few, NUREG-series publications; *Federal Register* notices; applicant, licensee, and vendor documents and correspondence; NRC correspondence and internal memoranda; bulletins and information notices; inspection and investigative reports; licensee event reports; and Commission papers and their attachments.

NRC publications in the NUREG series, NRC regulations, and *Title 10, Energy*, in the Code of *Federal Regulations* may also be purchased from one of these two sources.

1. The Superintendent of Documents
   U.S. Government Printing Office
   Mail Stop SSOP
   Washington, DC 20402–0001
   Internet: bookstore.gpo.gov
   Telephone: 202-512-1800
   Fax: 202-512-2250
2. The National Technical Information Service
   Springfield, VA 22161–0002
   www.ntis.gov
   1–800–553–6847 or, locally, 703–605–6000

A single copy of each NRC draft report for comment is available free, to the extent of supply, upon written request as follows:

Address: U.S. Nuclear Regulatory Commission
Office of Administration
Mail, Distribution and Messenger Team
Washington, DC 20555-0001
E-mail: DISTRIBUTION@nrc.gov
Facsimile: 301–415–2289

Some publications in the NUREG series that are posted at NRC's Web site address http://www.nrc.gov/reading-rm/doc-collections/nuregs are updated periodically and may differ from the last printed version. Although references to material found on a Web site bear the date the material was accessed, the material available on the date cited may subsequently be removed from the site.

Non-NRC Reference Material

Documents available from public and special technical libraries include all open literature items, such as books, journal articles, and transactions, *Federal Register* notices, Federal and State legislation, and congressional reports. Such documents as theses, dissertations, foreign reports and translations, and non-NRC conference proceedings may be purchased from their sponsoring organization.

Copies of industry codes and standards used in a substantive manner in the NRC regulatory process are maintained at—

The NRC Technical Library
Two White Flint North
11545 Rockville Pike
Rockville, MD 20852–2738

These standards are available in the library for reference use by the public. Codes and standards are usually copyrighted and may be purchased from the originating organization or, if they are American National Standards, from—

American National Standards Institute
11 West 42nd Street
New York, NY 10036–8002
www.ansi.org
212–642–4900

Legally binding regulatory requirements are stated only in laws; NRC regulations; licenses, including technical specifications; or orders, not in NUREG-series publications. The views expressed in contractor-prepared publications in this series are not necessarily those of the NRC.

The NUREG series comprises (1) technical and administrative reports and books prepared by the staff (NUREG–XXXX) or agency contractors (NUREG/CR–XXXX), (2) proceedings of conferences (NUREG/CP–XXXX), (3) reports resulting from international agreements (NUREG/IA–XXXX), (4) brochures (NUREG/BR–XXXX), and (5) compilations of legal decisions and orders of the Commission and Atomic and Safety Licensing Boards and of Directors' decisions under Section 2.206 of NRC's regulations (NUREG–0750).

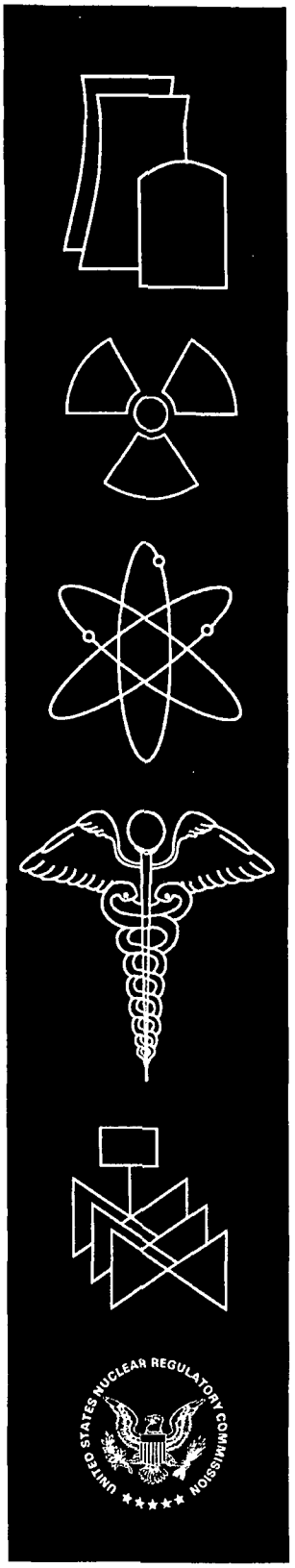

NUREG/CR-6935
ANL-04/04

Sensitivity Studies of Failure of Steam Generator Tubes during Main Steam Line Break and Other Secondary Side Depressurization Events

Manuscript Completed: December 2006
Date Published: May 2007

Prepared by
S. Majumdar, K. Kanza, J. Oras, J. Franklin, and C. Vulyak, Jr.

Nuclear Energy Division
Argonne National Laboratory
9700 South Cass Avenue
Argonne, IL 60439

E. Reichelt, NRC Project Manager

Prepared for
Division of Fuel, Engineering and Radiological Research
Office of Nuclear Regulatory Research
U.S. Nuclear Regulatory Commission
Washington, DC 20555-0001
NRC Job Code Y6588

Abstract

This report summarizes sensitivity studies conducted on the failure of flawed steam generator tubes in a Westinghouse Model 51 steam generator (SG) during main steam line break (MSLB) and feed water line break (FWLB) events. The results of thermal hydraulic transient analysis of temperature and pressure pulse loading during the MSLB and FWLB events were obtained from a recent Nuclear Regulatory Commission (NRC) report. A simplified but conservative finite element model of the tube support plates (TSPs) and their supports and SG tubes was used to analyze the loads transferred to the SG tubes from the TSPs during the transients. Fracture mechanics analyses were conducted to determine the stability of postulated cracks in the SG tubes on the top of the tube sheet and the TSPs. The potential for crack growth during repeated application of the pressure pulse was explored. Tests on SG tubes subjected to bending load and internal pressure showed that the effect of bending on burst pressure is negligible for the type of bending-to-direct-axial-stress ratio that is expected during a MSLB.

Foreword

This report discusses a study, conducted by Argonne National Laboratory (ANL), under contract to the U.S. Nuclear Regulatory Commission (NRC), Office of Nuclear Regulatory Research (RES), to assist the NRC's Office of Nuclear Reactor Regulation (NRR) in evaluating assessments of steam generator (SG) tube integrity. The purpose of this study was to evaluate the assertion that dynamic loads induced in SG tubes by a main steam line break (MSLB) or other secondary side breaches could lead to crack growth and increased SG leakage or ruptures. The concern is that during a transient, SG tubes, which are effectively locked to the tube support plates (TSPs), may experience loads transferred from those TSPs, and the transferred loads may challenge the integrity of the tubes.

To evaluate this assertion, ANL conducted finite element analyses to calculate the loads that are transferred to the SG tubes in the event of the transients of concern. Initially, ANL reviewed the related thermal-hydraulic analyses, which showed that the most critical transient is the large-break MSLB. ANL then conducted static-elastic finite element analyses of a Model 51 SG TSP, which included seven TSPs, supporting stay rods, wedges, and a small number of tubes that were locked to the TSPs. In so doing, ANL considered the "worst case" to be a scenario in which only a small number of tubes were locked to the TSPs. Consequently, ANL conducted analyses with 1, 2, 4, or 10 tubes per quadrant locked to the TSPs in a local region. Specifically, those analyses involved modeling the interaction created by locking the SG tubes to the TSPs. In so doing, ANL assumed that the tubes were fixed to the tubesheet, which was further assumed to be rigid. The transferred loads were calculated, and the resultant effects on various types of flaws were analyzed.

Overall, the experimental results revealed that even if only a few percent of the tubes in an SG are locked to the TSPs by crevice deposits or corrosion products, the loads associated with an MSLB or other secondary side breaches will have minimal impact on the integrity of SG tubes unless extensive circumferential cracking is present. In addition, the unit pressure drop analysis for each of the TSPs showed that the load was primarily transferred as a tensile axial load on the locked SG tubes. The analysis also showed that if 10 or more tubes are locked to the TSPs, the allowable throughwall circumferential crack in the tubes could be greater than 180 . Moreover, if all of the SG tubes were locked to the TSP, the allowable circumferential crack could be greater than 300 . In addition, the loads transferred to the tubes have virtually no effect on axial flaws in the SG tubes.

In addition to examining the effect of pressure loads, ANL conducted a fatigue analysis, considering that the TH results showed that at most one or two pressure pulse peaks occur during an MSLB transient. The fatigue analysis also showed that the average crack growth rate for a 100% throughwall circumferential crack is roughly 0.1 per cycle. Thus, if four SG tubes per quadrant were locked to the TSPs, throughwall circumferential cracks greater than 85 would not grow to failure. Moreover, with 10 tubes locked, this margin would be increased such that throughwall circumferential cracks up to 230 would not grow to failure. Therefore, given the nature of secondary side depressurization events, fatigue does not pose a concern.

Brian W. Sheron, Director
Office of Nuclear Regulatory Research
U.S. Nuclear Regulatory Commission

Contents

Figures

Tables

Executive Summary

Tube pull experience on a Model 51 steam generator (SG) with carbon steel tube support plates (TSPs) has shown that it often takes a fairly large force to remove the tubes from the TSP intersections, suggesting that the tubes are effectively locked to the TSPs. This report summarizes sensitivity studies conducted on the failure of flawed SG tubes in a Westinghouse Model 51 SG during main-steam-line-break (MSLB) and feed-water-line-break (FWLB) events. The concern is that, during transients, the Model 51 SG tubes, which are effectively locked to the carbon steel TSPs, may experience loads transferred from the TSPs that may challenge the integrity of tubes that contain cracks. The objective of this study was to review the literature that is pertinent to these transients; use, as much as possible, the information contained in the literature to carry out tube integrity analyses; and determine if more refined analyses are needed.

A review of the available thermal hydraulic (TH) analyses of MSLBs and FWLBs for the Westinghouse Model 51 and Model E2 SGs showed that the most critical transient from a SG tube integrity standpoint is the large-break MSLB event. During such an event, the pressure drops across the TSPs are the greatest. The lateral pressure load on the tubes is also greatest during a large-break MSLB, but the pressures are too low to cause significant bending stress (<1 ksi) in the tubes. It was shown that the periods of the fundamental vibration modes of the tubes and the TSPs are sufficiently short, when compared with the rise time of the pressure pulse during a MSLB, so the inertia effects can be ignored.

Static-elastic finite-element analyses of a Model 51 SG TSP, including the supports, and with and without a single tube (at the maximum displacement point) locked to the TSP, showed that the maximum TSP displacement under a unit pressure loading is reduced from 0.44 in. to 0.054 in. (11.2 to 1.4 mm), while the displacement of the tube at the TSP junction (which had been the maximum displacement point) is reduced to 0.013 in. (0.33 mm). These results are in agreement with industry reports, indicating that the axial stiffness of the SG tubes is far greater than the bending stiffness of the TSPs, whose stiffness is reduced significantly due to the presence of numerous tube holes and flow holes.

An earlier industry analysis of a Model 51 SG assumed that all of the tubes were locked into the TSPs. Comparisons of the resultant loads transferred from the plates to the tubes showed that they were relatively small when compared with the pullout forces measured on actual SGs.

To assess the "worst case" situations when only a small number of tubes are locked, a simplified but conservative finite-element model of the 7 TSPs of a Model 51 SG, including the supporting stay rods and wedges, was developed. The supporting rods and wedges were assumed to provide rigid support to the TSPs. Interaction between the TSPs was modeled by the locked SG tubes only. The tubes were assumed to be fixed to the tubesheet (TS), which was assumed to be rigid. Approximate analyses were carried out with 1, 2, 4, and 10 tubes locked to the TSPs in a local region. Unit pressure drop (upward) analyses for each of the TSPs in turn showed that the pressure load was primarily transferred as tensile axial load on the locked SG tubes below the loaded TSP, although ≈10-15% of the load was carried as axial compressive load in the tube sections above the loaded TSP. As expected, the axial load per tube decreased steadily as the number of locked tubes was increased. Also, the results

showed that the maximum bending stress in the tubes is much smaller than the maximum direct axial stress. Therefore, the tube integrity calculations were conducted for tubes under axial loading only. Tests conducted on SG tubes subjected to bending load and internal pressure showed that the effect of bending on burst pressure is negligible for the type of bending-to-direct-axial-stress ratio that is expected during a MSLB.

The results of the unit pressure drop analysis were used to calculate the axial loads that act on the various tube sections of the Model 51 SG under a large-break MSLB transient. The pressure drops associated with a MSLB in industry reports were compared with calculations performed with the NRC TH code, TRAC-M. The agreement among the various calculations is generally good. For the present calculations, the TRAC-M results were used, although the reported pressure drops were multiplied by an uncertainty factor of 1.5. In the case where only a few tubes are locked, initial analysis results showed that unrealistically large loads were transferred from the TSPs to the locked SG tubes if no consideration was given to the maximum pullout load capability of the tube-to-TSP joint. A review of tube pullout data from a retired SG from Dampierre, a French nuclear plant, showed that the mean value of the tube pullout load at operating temperature is 2.7 kips per tube per intersection and a reasonable upper bound (upper 95% confidence limit) is 4 kips per tube per intersection.

Reanalyses showed that, even when the maximum tube pullout capability was limited to more realistic values, the calculated axial tensile stresses on the locked tubes at lower elevations exceeded the ultimate tensile strength if only 1 or 2 tubes were assumed to be locked at the TSPs. Although this alone would not suggest rupture of the locked tubes if they were unflawed, it would imply that tolerance for circumferential cracks in these tubes could be severely limited. However, inasmuch as the mechanism for locking of the tubes to the TSPs is crevice corrosion within the TSPs, it is highly improbable that only 1 or 2 tubes out of more than 3000 tubes in the SG could be locked to the TSPs while the rest are free to slide. A more plausible assumption would be that multiple tubes, possibly 10 or more, in a local region are locked to the TSP. The analyses showed that, if 10 neighboring tubes are locked to each of the TSPs, the maximum axial load in the locked tubes is reduced significantly and the allowable throughwall (TW) circumferential cracks in the tubes at all of the TSP junctions would be $\geq 180°$. If all of the tubes are locked, the maximum tube axial load is 1.6 kips and the permissible crack length is $\geq 300°$. The loads transferred to the SG tubes during the transients have virtually no effect on the burst pressure and leak rate integrity of tubes with axial cracks.

Although the available TH results for the MSLB transient show at most 1 or 2 pressure pulse peaks, fatigue analyses were conducted to demonstrate that sufficient margin exists for crack growth in the event that the pressure drop pulses were to occur repeatedly. The fatigue analysis showed that the average crack growth rate for 100% TW circumferential cracks just before rupture is of the order of only 0.1°/cycle. With as few as 16 tubes locked (4 tubes/region), circumferential TW cracks that extend $\leq 85°$ would not grow to failure. With 40 tubes locked (10 tubes/region), cracks that extend $\leq 230°$ would not grow to failure. If the cracks are part-throughwall, even longer cracks can be tolerated.

The results of the present study show that, if even a few percent of the tubes in a SG are locked to the TSPs by crevice deposits or corrosion products, the dynamic loads associated with a MSLB will have little impact on the integrity of SG tubes unless extensive

circumferential cracking is present. Anecdotal evidence and the results of an extensive study on the pullout forces at Dampierre strongly support the conclusion that SGs with drilled-hole carbon steel TSPs will have enough tubes locked that the dynamic loads will be of little concern. Although there is limited pullout force data, measured values from US steam generators are comparable to those in Dampierre.

As noted previously, industry calculations obtained with RELAP5 for pressure drops across the TSPs due to a MSLB and U.S. Nuclear Regulatory Commission (NRC) staff calculations with TRAC–M give comparable results. In addition, bounding analyses of the pressure drops undertaken by both the industry and NRC staff give comparable results and are approximately a factor of 2 higher than the code calculations. Therefore, no further TH analysis is required.

Acknowledgments

The authors thank Dr. W. J. Shack of Argonne National Laboratory for helpful discussions, and Dr. W. Krotiuk of the Office of Nuclear Regulatory Research, U.S. NRC, for providing the analysis results. This work is sponsored by the Office of Nuclear Regulatory Research, U.S. NRC, under Job Code Y-6588; Project Manager: E. Reichelt.

Acronyms

ANL	Argonne National Laboratory
ARC	Alternate repair criteria
ASME	American Society of Mechanical Engineers
CANDU	Canadian Deuterium Uranium reactor
COA	Crack opening area
COD	Crack opening displacement
CTOD	Crack tip opening displacement
EdF	Electricitè de France
EDM	Electrodischarge machining
FDB	Flow distribution baffle
FEA	Finite-element analysis
FWLB	Feed water line break
MSLB	Main steam line break
NO	Normal operation
NRC	(U.S.) Nuclear Regulatory Commission
OD	Outer diameter
PTW	Part-throughwall
RT	Room temperature
SG	Steam generator
SLB	Steam line break
TH	Thermal hydraulic
TS	Tubesheet
TSP	Tube support plate
TW	Throughwall

Symbols

A	Cross-sectional area
a	Crack length
D	Bending stiffness
E, E_{eff}	Young's modulus and effective Young's modulus
h	Wall thickness
J, ΔJ	J-integral and range of J-integral
K, ΔK	Stress intensity factor and range of stress intensity factor
ΔK_J	Equivalent stress intensity factor range determined from ΔJ
K_{ax}	Axial stiffness
L	Span of beam
N	Cycles
R	Mean radius of tube
ν, ν_{eff}	Poisson's ratio and effective Poisson's ratio

1 Introduction

This report describes an assessment of the potential for rupture of tubes in a generic Model 51 steam generator (SG) because of tube support plate (TSP) displacement during a postulated main-steam-line-break (MSLB) or a feed-water-line-break (FWLB) event. The assessment is supported by finite element analyses (FEAs) based on structural analysis results reported in the past by Westinghouse in connection with various alternate repair criteria (ARC) in which the impacts of such accidents were evaluated[1,2].

The SG tubes pass through 7 TSPs, which provide lateral support to the tubes and contain circulation holes through which the water/steam passes upward through the tube bundle. During normal operation (NO), a slight pressure drop exists across each TSP. This pressure drop causes small displacements of the TSPs relative to the tubes if there are no contacts between the tubes and the TSPs. In hot-standby condition, there is no pressure drop across the TSPs. However, during a postulated accident condition (e.g., MSLB or FWLB), the pressure differentials across individual TSPs could act to displace the TSPs in the unsupported regions. These displacements would be resisted by the forces between the tubes and the plates because of deposits in the crevices between the tubes and the plates. Tube pullout experience on a Model 51 SG with carbon steel TSPs has shown that it often takes fairly large forces to remove the tubes from the TSP intersections, suggesting that the tubes are effectively locked to the TSPs. Operational assessments typically ignore these forces and assume that such displacements may uncover cracks under the TSPs. The tube integrity criteria used in the assessments are chosen to ensure the integrity of the tubes under pressure loads even if cracks are uncovered.

Although it is conservative to ignore the loads between the tubes and the TSPs when assessing the impact of pressure loads, the contact forces could apply significant axial and transverse loads to the tubes. These loads could make tubes that contain circumferential stress corrosion cracks either near the tube-to-TSP junctions or the tube-to-tubesheet (TS) junctions more susceptible to failure. The present report addresses the potential for immediate rupture and cyclic crack growth that leads to the rupture of these cracks because of such loads during a MSLB or FWLB event.

2 Background Information

Detailed thermal hydraulic (TH) analyses with RELAP 5, and dynamic structural analyses of a generic Westinghouse Model 51 SG during a postulated steam-line-break (SLB) event were reported in Ref. 1. Initially, transients that correspond to SLB, FWLB, and seismic events were considered, but it was concluded that a SLB event was the most limiting from the viewpoint of TSP transverse displacement. Therefore, SLB events that correspond to a small guillotine break (throat area = 1.4 ft^2) downstream of the flow restrictor, and a large guillotine break (throat area = 4.6 ft^2) upstream of the flow restrictor were analyzed. The objective of the report was to show that locking of the SG tubes to the TSPs (because of crevice corrosion) would prevent any relative displacement between the tubes and the TSPs, thus preventing the exposure of stress corrosion cracks in the SG tubes under the TSPs during the transients. In parallel with the detailed TH and dynamic structural analyses, results from actual tube pullout tests were presented and discussed to support the conclusions. The analysis methods and tube pullout tests will be discussed in a later section.

Additional TH analyses with RELAP 5 and dynamic structural analyses of a Westinghouse Model E2 SG during a postulated SLB and FWLB were reported in Ref 2. The results from these analyses were used to justify a 3-volt repair limit, because displacements in most of the TSPs were very small. The analysis methodologies followed in Refs. 1 and 2 are basically the same, although the SG configurations differ (Model E2 contains a preheater section, Model 51 does not). In both cases, the SLB events from hot standby were shown to be more limiting from the viewpoint of TSP displacement than either SLB from full power or FWLB.

Bhasin et al.[3] studied the effects of a MSLB or FWLB on SG internals of a Canadian Deuterium Uranium (CANDU) reactor. CANDU reactor SGs are similar in design to Westinghouse SGs. Dynamic structural analyses were conducted for 2 conditions: 100% FWLB at 100% power and 100% MSLB at hot standby (0% power).

The FWLB transient was analyzed to 500 ms and the MSLB transient, to 1000 ms. The SG contained ≈2489 U-tubes that were rolled and welded to the TS; they were supported at regular intervals by 13 grid spacers. The grid spacers, which provided lateral support to the tubes but allowed free movement in the axial direction, ignored stresses in the U-tubes that were a result of deformation of other SG internals and considered only the drag forces on the tubes during the transients. The maximum drag force per tube was calculated as 21.9 lbs/tube (0.63 kg (f)/tube) for the MSLB transient and 1.39 lbs/tube (0.63 kg (f)/tube) for the FWLB transient. The maximum stresses in the most highly stressed tube (V-72) were estimated as 1.9 ksi (134 kg (f)/cm^2) during a MSLB and 0.13 ksi (9.3 kg (f)/cm^2) during a FWLB, both of which are negligible when compared with the allowable stress intensity of 75 ksi (5298.3 kg (f)/cm^2). However, because no interaction (other than transverse constraint) between the grid spacers and the U tubes was considered, the results of this study are not applicable to our concern in this report.

2.1 NRC Staff Thermal Hydraulic Analyses

Krotiuk of the U.S. Nuclear Regulatory Commission (NRC) Office of Nuclear Regulatory Research reported results from detailed TH analyses of a generic Westinghouse Model 51 SG

that was subjected to a small- or large-break MSLB or a FWLB, by using the NRC TH Code TRAC-M.[4] The transients were calculated to 10 s. As in the other studies, the results show that a guillotine rupture of the steam line under hot-standby conditions produces the largest pressure loading on the TSPs.

The pressure drops across the TSPs for a large- and small-break MSLB from hot standby are shown in Figs. 1a and b, respectively. A positive pressure drop acts in the upward direction of the TSPs. Similar data for a FWLB from 100% full power and hot standby are shown in Figs. 2a and b, respectively. In contrast to MSLB, the pressure drops during FWLB from 100% full power are greater than those from hot standby.[4] The pressure drops during either a small- or large-break MSLB are much greater than those during a FWLB from full power.[4] Note that the peak pressure drops across the various TSPs do not all occur at the same time. The peak pressure drop may be followed by a second smaller peak, but in no case were additional cycles of any appreciable amplitude observed. The maximum pressure loads on the TSPs calculated by TRAC-M are close to the Westinghouse results obtained with RELAP5, as shown in Table 1.[1,4]

Krotiuk also reported the transverse pressure difference that acts on the SG tubes in the area below TSP1, where feedwater flow enters, and at the primary-tube U-bend.[4] The transient pressure loading that acts at the bottom during MSLB from hot standby and FWLB from full power are shown in Fig. 3. The loading at the SG bottom acts only on the bottom-most 14 in. (0.36 m) of the primary tubes. (The 14-in. [0.36-m] height is the distance between the bottom of the cylindrical shroud and the point of entry of the primary tubes; it represents the area where feedwater flow turns and enters the flow channel around the primary tubes.) A horizontal, radially inward-directed force at the SG bottom is defined as positive. A maximum pressure of –0.28 psi (-1930 Pa) occurs during a MSLB transient.

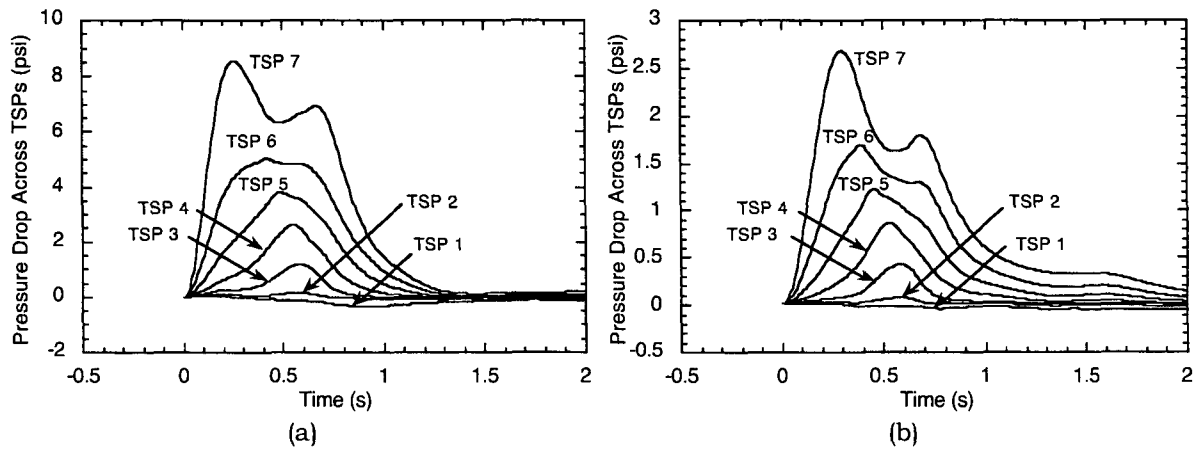

Figure 1. Variations of pressure drops across TSPs for (a) large-break (4.6 ft^2) and (b) small-break (1.4 ft^2) MSLB from hot standby. Note: 1 psi = 6.9 KPa and 1 ft^2 = 0.093 m^2.

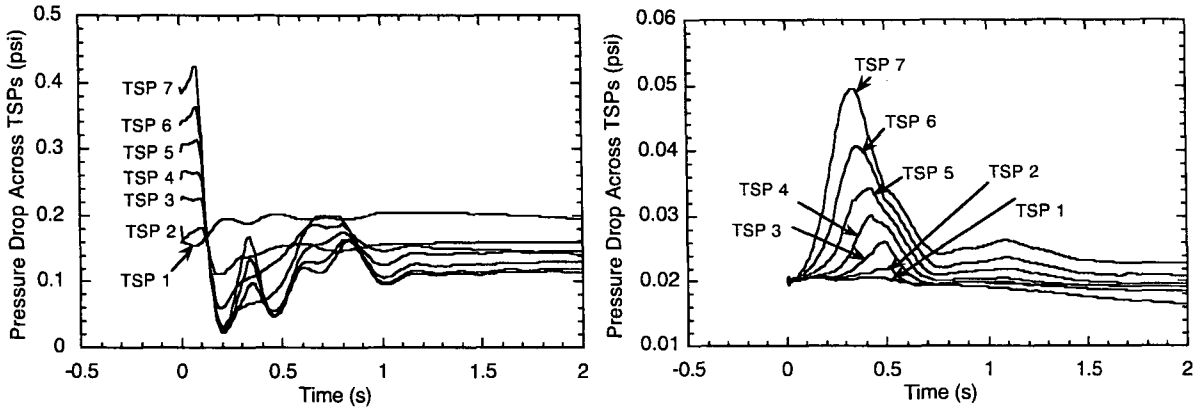

Figure 2. Variations of pressure drops across TSPs for FWLB from (a) 100% full power and (b) hot standby. Note: 1 psi = 6.9 KPa.

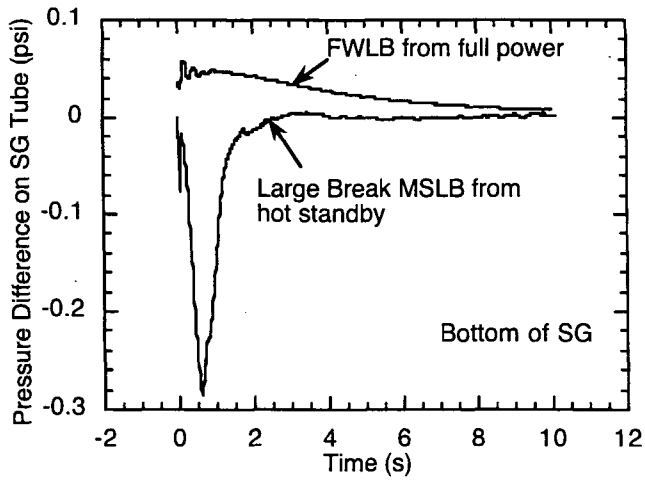

Figure 3. Pressure difference on SG tube at bottom of SG during MSLB and FWLB. Note: 1 psi = 6.9 Kpa.

Table 1. TSP peak differential pressures in psi (KPa) calculated by RELAP5 and TRAC-M for large-break (4.6 ft^2 [0.43 m^2]) SLB with system initially at hot standby.

TSP Number	RELAP5[a]	TRAC-M[b]
7 (top)	9.6 (66)	8.57 (59)
6	8.1 (56)	5.06 (35)
5	6.1 (42)	3.84 (26)
4	4.5 (31)	2.63 (18)
3	3.2 (22)	1.16 (8)
2	2.0 (14)	0.15 (1)
1 (bottom)	1.9 (13)	-0.33 (-2)

[a]From Ref. 1.
[b]From Ref. 4.

3 Review of Industry Analyses

3.1 Results for Model 51 SG (WCAP-14707)

Each Westinghouse Model 51 SG (Fig. 4) contains more than 3000 mill-annealed Alloy 600 U-tubes with 0.875-in. (22.2-mm) OD and 0.050-in. (1.27-mm) wall thickness. The SG tubes pass through 7 TSPs, which provide lateral support to the tubes and contain circulation holes through which water/steam passes upward through the tube bundle. The TSPs are 0.75-in. (19 mm)-thick carbon steel plates with round drilled 0.891-in. (22.6-mm)-diameter tube holes (nominal radial clearance = 0.008 in. [0.2 mm]) set on a square pitch of 1.28 in. (32.5 mm). The TSPs also contain 0.75-in. (19-mm)-diameter flow circulation holes on a square pitch of 1.28 in. (32.5 mm) within the tube hole array.

The TSPs are supported vertically by a central tierod/spacer and 4 outer tierod/spacers near the edge of the plate. Tierods are bars that are threaded into the TS and run the full length of the tube bundle; a nut is welded to both the tierod and the top surface of the TSP on the upper side of the top TSP. Hollow, cylindrical spacers are placed over the tierods and are located between each of the TSPs for positioning purposes. The spacers on the central tierod are welded to each TSP, with the exception of the spacer between the TS and the first TSP; this spacer is not welded to the TS. For the spacers around the periphery of the TSPs, no rigid link is provided between the spacers and the TSPs. Therefore, the interface behavior may be nonlinear, i.e., it can transfer compressive load but could open up under tensile loading. However, in the analysis presented in Ref. 1, it was assumed that TSPs do not separate from the spacers because of tight tube/plate interfaces. A nonlinear interface was considered only for the spacer between the TS and the first TSP.

In-plane support of the TSPs is provided by tapered wedges that are around the periphery of each plate. The wedges are welded to both the wrapper and the TSP on both top and bottom surfaces. Thus, the wedges also restrain vertical motion of the TSPs. Finally, 2 bar supports are welded, 180° apart, between each TSP and the wrapper.

In the analysis, the material properties (e.g., Young's modulus, Poisson's ratio, and mass density) of the TSPs were modified to account for the tube holes in the TS and both the tube holes and flow holes in the TSPs. In the finite-element analysis (FEA), a 90° segment of the SG was modeled. The 1694 tubes were divided into 30 groups of tubes; each group was modeled by a beam with cross-sectional properties equal to the number of tubes included in each group. The assumption was made that all of the tube intersections were dented or packed, i.e., the plates were displaced with the tubes, and exhibited a much higher stiffness than the transverse stiffness of the TSPs. Thus, the dynamic response of the system was reduced to the tube bundle mode. In fact, most of the pressure load acting on the TSPs was carried by the locked tubes. The fundamental frequency of the tube bundle was determined to be 84.5 Hz. Because the objective of the study was to define the magnitude and distribution of tube/TSP interface loads required to produce the tube bundle mode, it was necessary that the tube/TSP intersection remain intact for the duration of the transient. Thus, for the analysis, an arbitrarily high breakaway force of 200 lbs (890 N) per tube was specified. The actual forces required to maintain the rigidity of the bundle were then calculated as part of the analysis.

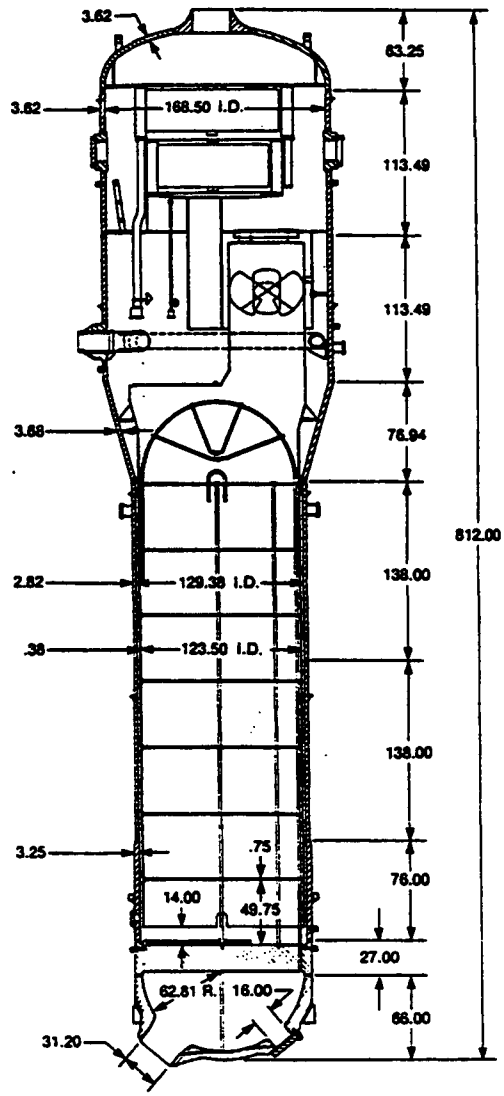

Figure 4. Model 51 steam generator layout.

3.1.1 Pressure Drop Results

In the Westinghouse analysis, the peak differential pressures acting on the various TSPs during the large-break transient are calculated by RELAP5. In Table 1 the RELAP5 calculations are presented with the NRC staff calculations, which were performed with TRAC-M. In all cases, the pressure differentials calculated by RELAP5 are greater than those calculated by TRAC-M. Results from dynamic structural analysis that correspond to the temperature and pressure loading calculated by RELAP5 are reported in Ref. 1. The variation in pressure drop with time (Fig. 5) showed a single cycle with a high peak, together with a few

additional cycles at much reduced amplitudes. Similar behavior was also reported by Krotiuk[4] for a limited long-term (60-s) analysis of the transient. Inasmuch as the large-break SLB produces greater pressure drops across the TSPs than either the small-break SLB or the FWLB, results from the large-break SLB analysis are used as the base case in the current assessment.

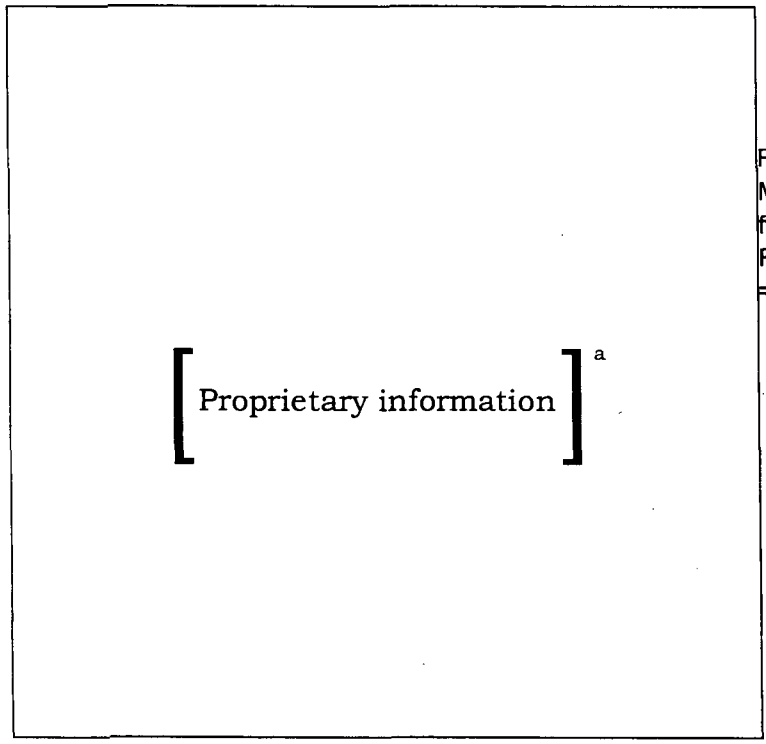

Figure 5. TSP pressure drops in a Model 51 SG for large-break SLB (4.6-ft^2) event, calculated by RELAP5. From Ref. 1. Note: 1 psi = 6.9 KPa and 1 ft^2 = 0.093 m^2.

3.1.2 Results of Load and Displacement Analysis

Because the wedges at the boundary are not located symmetrically with respect to the SG axes, 2 geometries were considered in the solutions. The first used the geometry of Quadrants 1 and 3, the second, the geometry of Quadrants 2 and 4. These geometries were assumed to give a bounding set of conditions for evaluating the dynamic solution. To account for the tube holes and flow holes, effective properties for Young's modulus [Proprietary information]^a, compared with 26 x 10^6 psi [179 GPa] for the carbon steel material), Poisson's ratio, and mass density were determined by conventional methods for the analysis of perforated plates. In addition, the density was modified to account for the added mass of the secondary-side fluid. The transient dynamic analysis was conducted with a time step of 0.0002 s and a structural damping of 4%.

Because of the locking effect of the tubes, the displacements of all of the TSPs relative to the installed positions essentially followed the displacement of the TS. The relative tube/TSP displacements due to stretching of the tubes varied between 0.0069 and 0.0134 in. (0.18 and 0.34 mm), as shown in Table 2. The maximum tube/TSP interaction forces for the large-break SLB loading are summarized in Table 3. Relative tube/TSP displacements would occur if these forces exceeded the breakaway forces for tube-to-TSP crevices. The maximum

values of the forces transferred to the tube from the TSPs (Table 3) are much less than the typical breakaway forces observed in tube pullout tests, as will be discussed in Section 5.

The total tube stress is the sum of the transient stress during a SLB plus the axial stress due to the internal pressure differential acting during the SLB event on a U bend tube (referred to as the "end-cap pressure stress"). The calculated stresses are tabulated in Table 4. The end-cap pressure stresses are much greater than the maximum values of the transient dynamic stresses. This is not surprising when one considers the fact that all of the tubes are locked at all of the tube/TSP intersections.

The ability of the tubes that contain stress corrosion cracks to carry these axially transmitted loads will be discussed in Section 6.

Table 2. Relative tube/TS displacements with respect to time = 0 for a large-break SLB.

TSP	Quadrant 1, 3 in. (mm)	Quadrant 2, 4 in. (mm)
[	Proprietary information	]a

Table 3. Summary of maximum tube/TSP interface forces in lbs (N) for a large-break SLB

TSP	Quadrant 1, 3	Quadrant 2, 4
[	Proprietary information	]a

Table 4. Summary of stresses in ksi (MPa) due to large-break SLB at support locations

TSP	Tube stress	End-cap stress	Total stress
[	Proprietary information		]a

3.2 Results for Model E2 SG (WCAP-15163)

The Westinghouse Model E2 preheat SG (Fig. 6a) originally at South Texas Unit 2 contains more than 4800 mill-annealed Alloy 600 U-tubes with 0.75-in. (19-mm) OD x 0.043-in. (1.09-mm) wall thickness. The structural dynamic analysis procedure reported in WCAP-15163 is similar to that used for analyzing the Model 51 SG in WCAP 14707.[1,2] The important difference is the presence of a preheater region in the Model E2 SG. The associated asymmetry makes the TH analysis and structural dynamic analysis more complex than the analysis of Model 51 SG. First, instead of modeling a quarter of the SG, it was necessary for Westinghouse to model one half of the SG by FEA (Fig. 6b). Also, in contrast to WCAP-14707, the junction between the tubes and the TSPs were assumed to be freely sliding in WCAP-15163. Because the TSPs in the South Texas SG are ferritic stainless steel, the likelihood of locking of the tubes in the TSP is significantly less than in the case of Model 51 SGs, in which the TSPs are carbon steel. The objective was to show, by analysis, that during an SLB or FWLB event, the displacements of the TSPs relative to the tubes are not sufficiently large to uncover potential stress corrosion cracks under the TSPs.

The Model E2 SG contains 10 TSPs, designated as C (bottom), F, J, K, L, M, N, P, Q, and R (top); 1 flow distribution baffle (FDB) A (9 in. above the TS); and 5 baffle plates in the preheater section, designated as B, D, E, G, and H. The plates are 0.75 in. (19 mm) thick, except TSP R, which is 1.12 in. (28 mm) thick; with the exception of the FDB and the baffle plates, they contain nominally 0.776-in. (19.7-mm)-diameter tube holes set on a square pitch of 1.08 in. (27.4 mm), and 0.5-in. (12.5 mm)-diameter circulation holes set on a square pitch of 1.08 in. (27.4 mm) within the tube array hole. The FDB and preheater baffle plates in the cold-leg side contain tube holes but no circulation holes (the purpose of the baffle plates is to direct the flow across the tubes). The preheater section is separated from the hot-leg side by a divider plate, located on the centerline of the SG, that extends from the elevation of Plate B to Plate L. Above Plate L, the cold leg and the hot leg are not physically separated. The Model E2 SG at South Texas Unit 2 utilizes Type 405 stainless steel TSPs with round drilled tube holes.

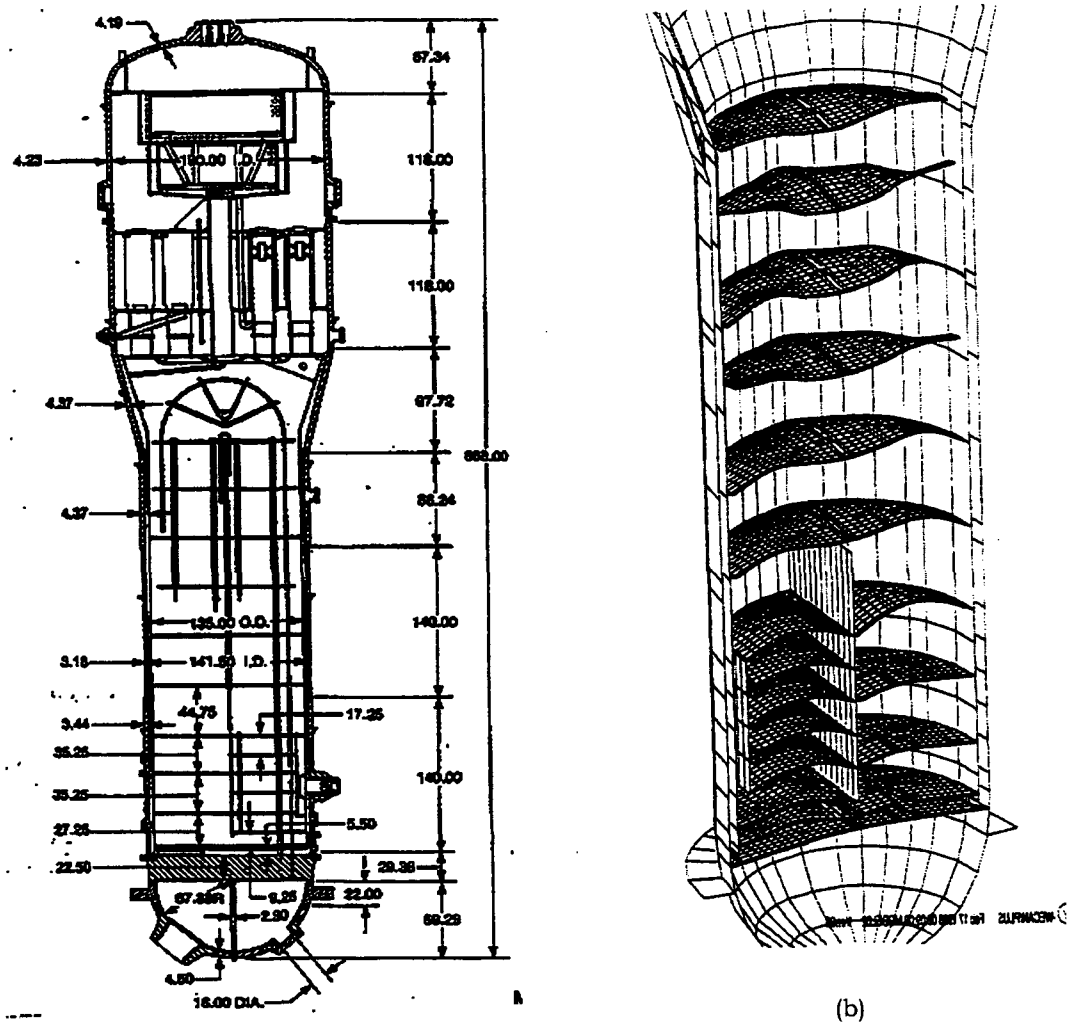

Figure 6. (a) Layout and (b) finite-element model of Model E2 SG (from Ref. 2).

The FDB, TSPs, and preheater baffle plates are supported vertically by several structural elements, including 7 tierods/spacers in each half of the tube bundle. Preheater baffles are supported by 18 additional stayrods. In addition, the plates are supported by vertical bars, located above and below the plates, welded to the wrapper or divider plate. Welded wedges around the circumference of each plate provide in-plane support. The tapered design of the wedges provides additional resistance to upward motion of the plates.

The results of TH analysis reported in WCAP-15163 were obtained by using RELAP5. As in the case of the Model 51, the pressure drops across the TSPs were higher for a SLB from hot standby than for a SLB from full-power operation. The time histories of pressure differentials across the various hot-leg TSPs during a SLB from hot standby are plotted in Figs. 7a and b. The pressure differentials are lower than calculated for Model 51 (Fig. 5). However, as in the case of Model 51, the TSPs at the higher levels experience consistently higher pressure differentials than the lower TSPs in the hot-leg side. The pressure differentials across the lower TSPs show a change in sign (flow reversal) during the transient. As before, at

most 2 major pressure cycles occur, with additional cycles occurring at smaller pressure amplitudes.

Using effective plate properties, such as Young's modulus, Poisson's ratio, and density (to account for added mass of the secondary side fluid), Westinghouse conducted transient dynamic finite-element structural analyses. A summary of the maximum/minimum displacements during the SLB transients from hot standby and full power are given in Table 5. Positive relative displacements are vertically upward, and are higher for a SLB from hot standby than for a SLB from full power, as expected. The last column in Table 5 includes the additional thermal effects in going from full power to hot standby.

Because of the uncertainties in the TH analysis due to mixing of the hot-leg flow with the cold-leg flow above Plate L, in an addendum to WCAP 15163, Westinghouse reported an independent bounding analysis of the pressure loads. The maximum bounding pressure differential was calculated to be 3.56 psi (24.5 KPa) at Plate R. For comparison, the maximum pressure drop calculated by RELAP5 earlier was 1.67 psi at the same TSP. Their analysis showed that, even under the bounding loads, the maximum relative tube/TSP displacement can be kept within acceptable limits by hydraulically expanding 16 tubes in the hot leg of each of the TSPs C, F, and J to lock the TSPs in place. A significant body of tube pullout force data were included in the report and the data are summarized in Section 5 of this report.

[Proprietary information] [a]

(a) (b)

Figure 7. Pressure differentials across (a) lower TSPs and (b) higher TSPs of a Model E2 SG during SLB from hot standby (from Ref.2). Note: 1 psi = 6.9 KPa.

Table 5. Summary of maximum/minimum tube/TSP relative displacements in in. (mm) during SLB

Hot leg TSP	SLB from hot standby	SLB from full power	Full power to hot standby + SLB
[	Proprietary information		]a

A stiffness value of [Proprietary information]a was used for each expanded joint when the restraining effect of the expanded tubes was incorporated in the structural model. Using static analysis with unit pressure loading, Westinghouse showed that the maximum tube-to-plate relative displacement could be reduced from 0.0808 in. (2.05 mm) (with no tube locked) to 0.0135 in. (0.34 mm) by placing 16 (out of more than 4800 tubes) expanded tubes strategically in the hot leg at each of TSPs C, F and J. The maximum pullout force on the locked tubes was calculated as <1 kip (4.45 KN) when all 3 TSPs were loaded by the bounding pressure differential of 3.56 psi (24.5 KPa). The pressure differential required to cause yielding in the maximally stressed locked tube was 13.3 psi (91.7 KPa) if a single plate was loaded, and 4.59 psi (31.6 KPa) if all 3 TSPs were loaded simultaneously. The single-plate loading was claimed to be more realistic because TH analyses generally show that the peak pressures are not reached simultaneously in all of the TSPs. Because the maximum bounding pressure load is 3.56 psi (24.5 KPa), these results suggest that the loads in the locked tubes will remain below yield during a MSLB.

3.3 Conclusions from Industry Analyses

The TSP pressure drops calculated by RELAP5 for the Westinghouse Model 51 SG under a SLB transient are comparable to but slightly larger than those calculated by TRAC-M. Both analyses identify the large-break (4.6 ft^2 [0.43 m^2]) SLB transient from hot standby as the most critical transient because it leads to significantly higher pressure drops across TSPs than either a SLB from full power or a FWLB. Both analyses show that each TSP experiences a single pressure drop peak, whose magnitude increases with the height above the TS from TSP 1 to TSP 7. However, all of the peak pressure drops may not occur at the same time. The large peak is sometimes followed by a second smaller peak and a few additional minor pressure cycles. Transient dynamic structural analyses were conducted only for the case when all of the TSP-to-tube junctions were locked by crevice corrosion. Under this constrained deformation mode, the highest SG tube stresses (including end-cap pressure stresses) remain <12.25 ksi (84.5 MPa), which corresponds to an axial load of 1.6 kips (7.1 KN).

The largest pullout force on any TSP that is required to maintain the constraint is 60 lbs (267 N), which, as will be discussed in Section 5, is much less than the typical tube-to-TSP junction breakaway force measured in the field for this type of SG.

The static structural analyses for the Model E2 SG, although not directly applicable to Model 51, show that, if a relatively few (16) SG tubes are locked to 3 lower TSPs by hydraulically expanding the tubes, the maximum tube/TSP relative displacement under a conservative bounding pressure drop loading can be reduced from 0.0808 to 0.0135 in. (2.05 to 0.34 mm) This is a direct consequence of the fact that the TSPs contain many tube and flow holes that reduce the effective stiffness of the TSPs to a value much less than the stiffness of the SG tubes. The maximum tube stress (27 ksi [186 MPa], corresponding to an axial load of 2.6 kips [11.6 KN]) remains less than yield even if all 3 TSPs that contain the locked tubes are loaded simultaneously under a bounding maximum pressure load. The maximum pullout load on the locked tubes was <1 kip (4.45 KN).

Taken together, both of the above analyses suggest that, if the number of locked tubes is sufficiently large, the pullout forces will be low when compared with those expected in SGs with drilled hole support plates, and the tube stresses will remain below yield. The number of locked tubes needed to ensure this outcome for the Model E2 SG appears to be approximately 16, which is a small fraction of the total number of tubes in the SG. The analyses available for the Model 51 SG do not directly address this particular problem, but it is expected that the number of locked tubes will again be a small fraction of the total number of tubes. Clearly, the most critical case for an SG would be one in which a single tube is locked at the TSP and all the remaining tubes are free to slide at the TSP junctions. In Section 4, the loads on tubes for cases in which only a very small number of tubes are locked are determined.

4 Supplementary Finite Element Analyses of Tube Loads

4.1 Transverse Pressure Loading on SG Tubes

The fundamental frequency of the bending vibration of the Model E2 SG TSPs is of the order of 40 Hz. The fundamental frequency of the tube bundle of the Model 51 SG is higher [Proprietary information][a] because all of the tubes are assumed to be locked to the TSPs and the tubes are much stiffer than the TSPs. The rise time for the pressure loading is >0.2 s (Figs. 1 and 3), which is much larger than the rise time for the fundamental vibration mode. Thus, inertia effects should not play a critical role in the stress and displacement analyses during a MSLB. If inertia effects are to be significant at all, they should occur during the transverse bending vibrational mode of the SG tube. The maximum transverse pressure loading on the SG tube has been calculated to occur between the TS and the first TSP during a MSLB (Fig. 3). Therefore, we conducted a transient dynamic analysis (no damping) of this span of the SG tube, using an idealized triangular pressure loading with a maximum pressure difference of 1 psi (Fig. 8). The variation of maximum bending moment with time is shown in Figs. 9a and 9b for rise times of 0.01, 0.02, and 1 s. It is clear that, unless the rise time for the pressure pulse is much shorter than 1 s, inertia effects are negligible. The peak bending stress that corresponds to the pressure pulse of Fig. 3 is only 775 psi (5.34 MPa).

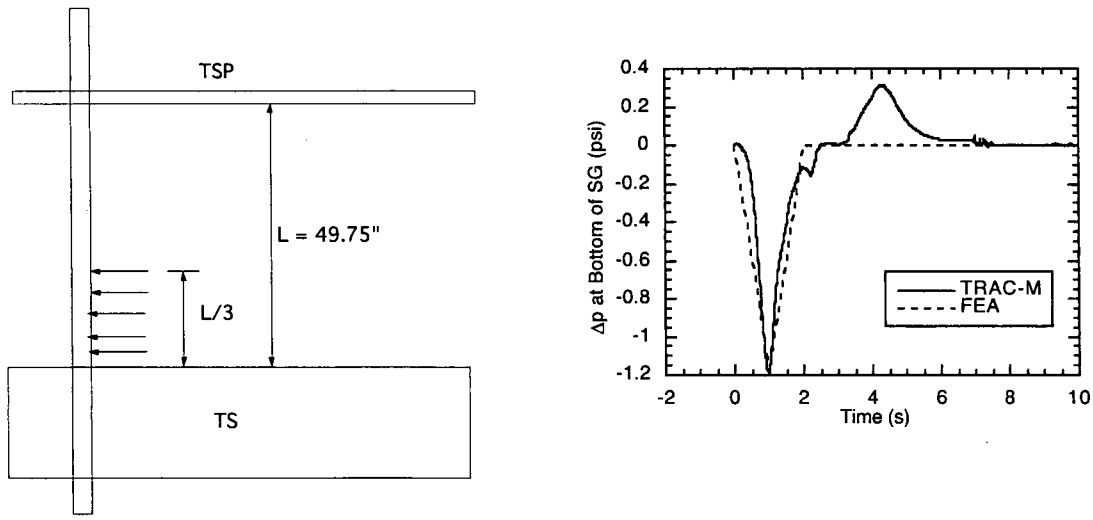

Figure 8. Transverse pressure differential loading on SG tube below the first TSP during MSLB. Note: 1 in. = 25.4 mm and 1 psi = 6.9 KPa.

4.2 Transverse Pressure Loading on TSPs

Because inertia effects are expected to be small, we initially conducted a series of static-elastic FEAs to explore the effect of 1, 2, or 4 SG tubes locked at the TSPs of a Model 51 SG during a large-break SLB transient. The pressure drops shown in Fig. 1a were used after multiplying them by a safety factor of 1.5, as recommended in Ref. 4. A quarter (Quadrant 1) of the 7 TSPs were modeled with tierods and wedge group supports, as shown in Figs. 10a and 10b. The supports were assumed to be rigid and the transverse displacement of the TS was ignored. These assumptions are conservative with respect to the tube stresses. Shell

elements were used to model the TSPs, and beam elements were used for the SG tubes. To model the locking of the tubes to the TSPs, we coupled all of the degrees of freedom for displacements and rotations of the TSPs and the SG tube at the intersections. Note that no stiffness value was attached to the tube-to-TSP joints per se (in other words, the stiffness constants for the locked joints was assumed to be infinity). Again, this assumption is conservative from the standpoint of tube stresses. The effective Young's modulus and Poisson's ratio of the TSPs, obtained from Ref. 1, were E_{eff} = 1.76 x 10^6 psi (12 GPa) and ν_{eff} = 0.5177, respectively. The Young's modulus and Poisson's ratio for Alloy 600 tubes were taken as E = 29 x 10^6 psi (200 GPa) and ν = 0.3. The transverse stiffness due to a point load at the center of a simply supported circular plate of radius R and thickness h is

$$D = \frac{16\pi(1+\upsilon_{eff})E_{eff}h^3}{12(1-\nu_{eff}^2)(3+\nu_{eff})R^2}. \tag{1a}$$

Using the TSP thickness h = 0.75 in. (19 mm) and the effective (the central tie rod/spacer cuts the effective radius of the TSP into approximately half) R = 62/2 = 31 in. (0.78 m),

$$D = 2 \text{ kips/in. (333 kN/m)}, \tag{1b}$$

The axial stiffness of the 7/8-in. (22.2-mm)-diameter and 0.05 in. (1.3 mm) wall thickness SG tube is

$$K_{ax} = \frac{EA}{L} = 75 \text{ kips / in. (13134 kN/m)}, \tag{1c}$$

where the cross-sectional area A is 0.13 in.^{2} (8.39 mm^2) and the span L which is the spacing between the TSPs is 50 in. (1.27 m). The rotational bending stiffness of the same plate due to a uniformly distributed bending moment around its periphery is given by

$$D_{rot} = \frac{E_{eff}h^3}{12(1-\nu_{eff})R} = 4 \text{ in–kips/in–rad (18 kN–m/m–rad)} \tag{1d}$$

Since the pitch of the SG tubes is 1.28 in. (3.3 cm), the rotational bending stiffness of the TSP per tube around the periphery is

$$D_{rot} = 5 \text{ in-kips/rad/tube (0.6 kN-m/rad/tube)}. \tag{1e}$$

For comparison, the rotational bending stiffness of a single tube clamped at one end and simply supported at the other is

$$K_{bend} = \frac{4EI}{L} = 26 \text{in–kips/rad (3 kN-m/rad)} \tag{1f}$$

where I is the moment of inertia of the tube cross-section. Equations 1b and 1c show that the axial stiffness of the tube is ≈ 40 times the transverse stiffness of the TSP and Eqs. 1e and 1f show that the rotational bending stiffness of the tube is ≈ 5 times the rotational bending stiffness of the TSP. Note that when the tubes are locked to the TSP, the maximum transverse displacement of the TSP occurs at a point where its rotation is small.

Before computing the displacements and forces due to the transient pressure drops acting on all of the TSPs (Fig. 1a), we analyzed a series of unit pressure loading cases in which each of the TSPs, in turn, was subjected to a unit pressure loading while the others were unloaded. The principle of superposition was then used to calculate the maximum displacements and forces due to the pressure loading on all of the TSPs.

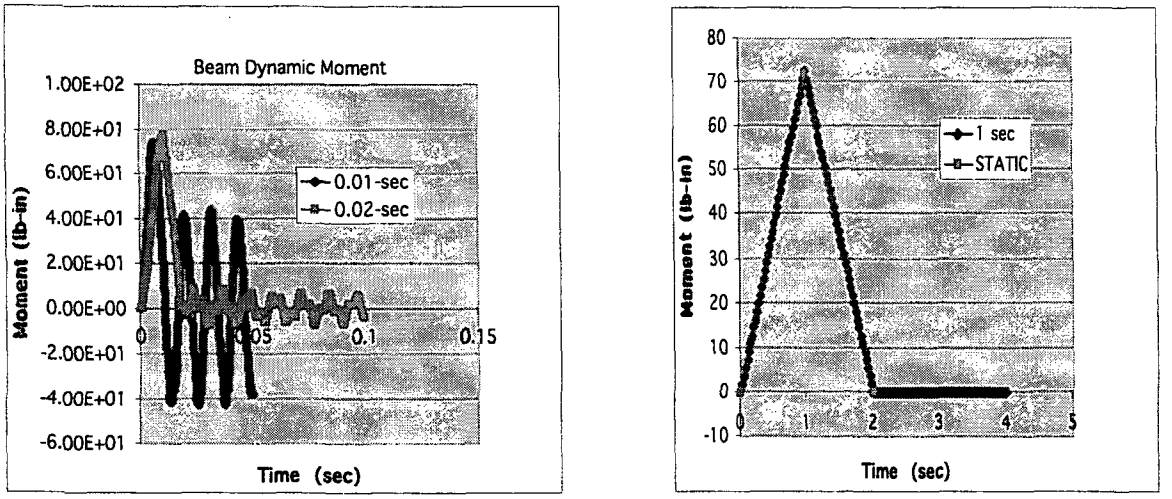

(a) (b)

Figure 9. Variation of maximum bending moment with time for triangular pressure pulse for rise times of (a) 0.01 and 0.02 s and (b) 1 s. Note: 1 lb-in = 113 N-mm.

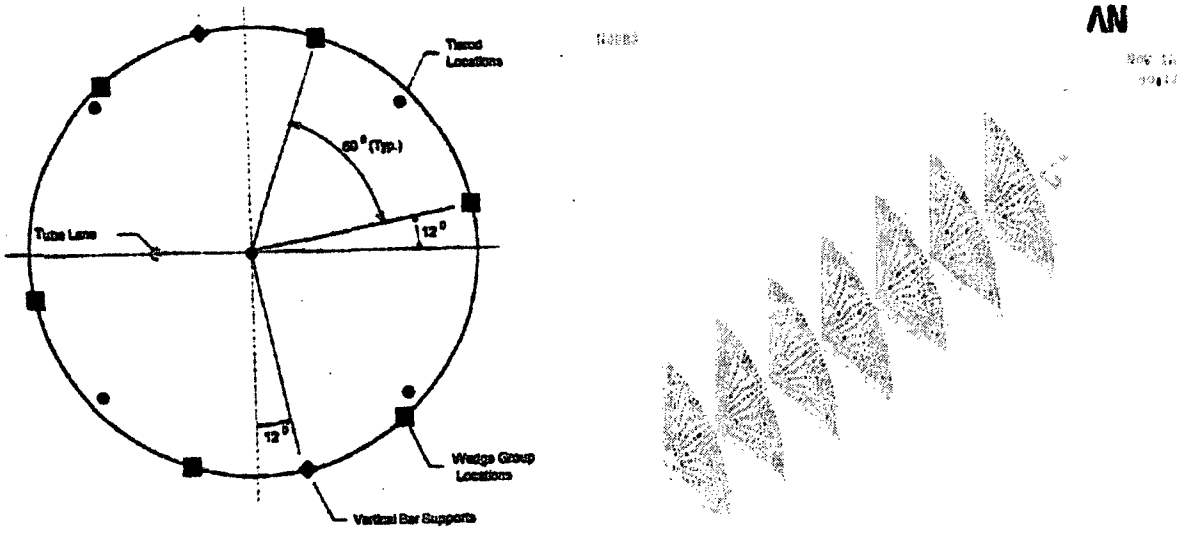

(a) (b)

Figure 10. (a) TSP support locations for a Model 51 SG and (b) finite-element model of a quarter (1st quadrant) of 7 TSPs and a locked single steam generator tube at point of maximum displacement.

4.2.1 Results from Unit-Pressure-Drop Analyses

Figure 11a shows the displacement along a 45° radial line (Fig. 10a) in the first quadrant of the unit-pressure-loaded first TSP when all of the SG tubes are freely sliding. If 1 tube at the TSP junction located at the maximum displacement point is locked, the displacements are drastically reduced, as shown in Fig. 11b. The maximum displacement is reduced from 0.44 in. to 0.054 in. (11.2 to 1.37 mm), while the displacement where the tube is locked is reduced to 0.013 in. (0.33 mm). The maximum von Mises effective bending stress in the plate is reduced from 7 to 3 ksi (48.3 to 20.7 MPa). These stresses are average stresses, which must be multiplied by a stress concentration factor to obtain the actual stresses in the narrow ligaments between the holes in the TSPs.

The axial load variation in a single SG tube (per quarter of a TSP) that is locked at every TSP junction is shown in Fig. 12a. Each line in this figure represents the axial load in the locked tube from unit pressure loading on the respective TSP. The corresponding direct and bending stresses are shown in Fig. 12b. Note that significant fractions of the pressure loading on the TSPs at higher elevation are passed on as axial tensile load on the SG tube at lower elevations. The maximum load carried by the locked SG tube just below TSPs 1 and 7, when they are loaded, is approximately a third of the total pressure loading (3 kips [13.3 KN]) on the modeled quarter of the TSPs and the rest is carried by the other support structures. Small fractions of the pressure loading on the lower TSPs are passed on as small compressive loads and stresses on the SG tube at higher elevations. Also, note that the maximum bending stresses are small when compared with the maximum direct tensile axial stresses. The effect of bending stresses on tube rupture was investigated both analytically and experimentally and the results are included in Appendix A. The results showed that the bending stresses for rupture analysis of the SG tube are negligible because they are small compared to the axial stresses.

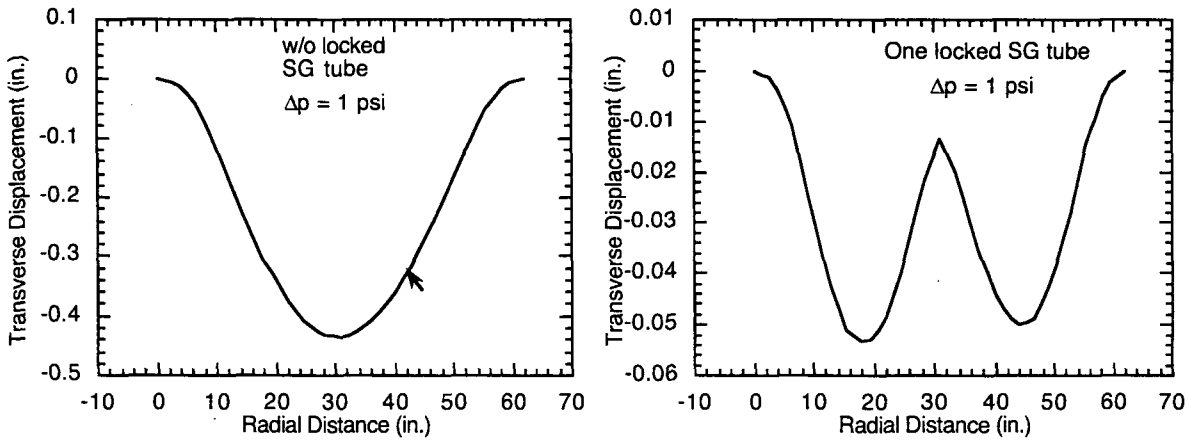

Figure 11. Radial variation of transverse displacement of TSP 1 due to 1-psi (6.9-KPa) pressure drop loading of a Model 51 TSP 1 when (a) all tube-to-TSP junctions are free to slide and (b) only 1 tube at the maximum displacement point is locked at TSP 1. Note: 1 in.= 25.4 mm.

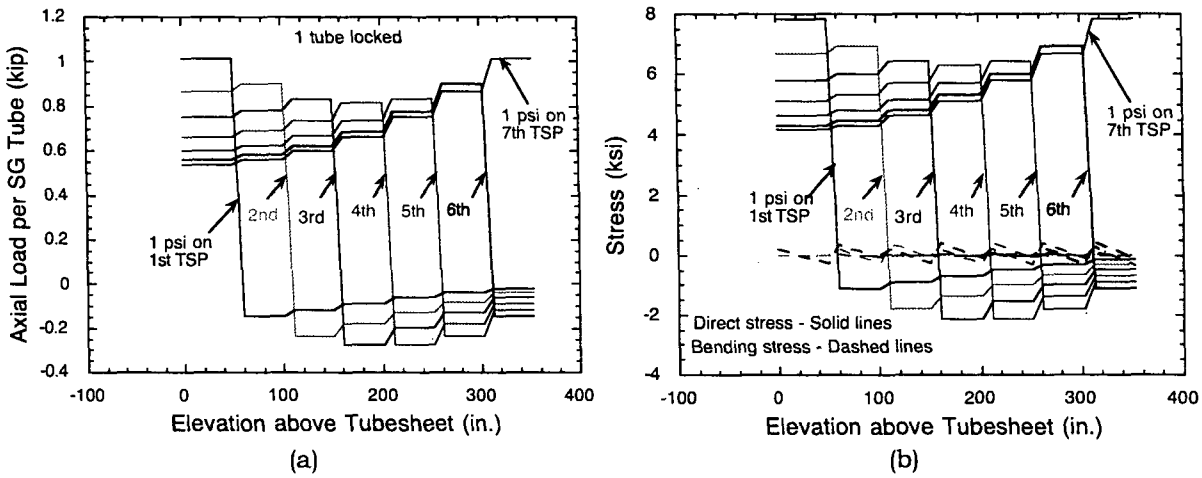

Figure 12. Variation of (a) axial load and (b) direct and bending stresses in a single locked tube in Model 51 SG for unit pressure loading cases. Note: 1 in.= 25.4 mm, 1 kip = 4.45 KN, 1 ksi = 6.9 MPa.

In reality, it is highly unlikely that a single tube out of more than 3000 tubes will be locked at the TSPs. Inasmuch as locking occurs because of TSP crevice corrosion, multiple-tube locking in a local region is more likely. Therefore, analyses were conducted for the cases where 2 and 4 tubes in a local region were locked to the TSPs. The case of 2 locked tubes was modeled by placing the second tube at the nearest plate node ≈3 in. away from the first. The axial load per tube is reduced significantly when 2 tubes are locked to the TSPs, as shown in Fig. 13a. The case of 4 locked tubes was simulated by doubling the cross-sectional areas of the 2 locked tubes. The results, plotted in Fig. 13b, show that, when compared with the case of 2 locked tubes, the axial loads are almost halved.

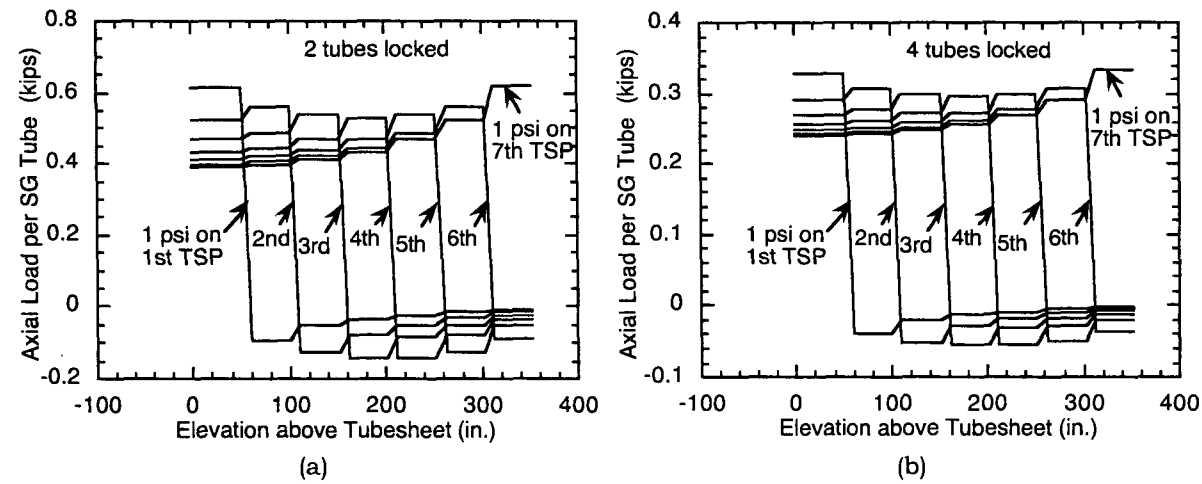

Figure 13. Variations of axial load per SG tube with (a) 2 tubes and (b) 4 tubes locked to TSPs for unit pressure loading cases. Note: 1 in.= 25.4 mm, 1 kip = 4.45 KN, 1 psi = 6.9 KPa.

Calculations showed that the maximum von Mises effective bending stress in the loaded plate in all 3 cases is ≈3 ksi (20.7 Mpa) which is much lower than the yield strength. The

maximum bending stress in the next neighboring unloaded plate is only 0.1 ksi (0.69 MPa). Thus, the elastic assumption for the TSPs is reasonable.

4.2.2 Results for the Large-Break MSLB Transient

The results for the large-break MSLB are obtained from the results of the unit load results after multiplying them by the actual pressure drops across the TSPs. Note from Fig. 1a that, although all of the peak pressures on the plates do not occur at the same time, each plate exhibits a nonzero pressure drop at the time peak pressure is reached in any particular TSP. Also, the pressures in Fig. 1a were multiplied by an uncertainty factor of 1.5.

Results for No Slippage between TSPs and a SG Tube

Variation of maximum total axial load in the locked SG tube at various TSPs is shown in Fig. 14a. Note that the maximum tube axial loads at each of the TSPs are not necessarily reached all at the same time, as shown in Fig. 1a. For example, the maximum axial load at TSP 6 has contributions from the maximum pressure loading on TSP 6 as well as the axial loads transferred from the pressure loadings on all the other TSPs occurring at the same time. For reference, the axial load needed to cause yielding in the SG tube is ≈5.4 kips (24 KN). Significant yielding will occur in the tube if only 1 or 2 tubes are locked at all of the TSPs, provided no slippage occurs between the tube and the TSPs.

The maximum values of the loads transmitted from the various TSPs to the locked tubes (the pullout loads) are shown in Fig. 14b. Continuing with the example of TSP 6 in the previous paragraph, the tube pullout load at TSP 6 is calculated using equilibrium of forces which requires that the load transmitted from TSP 6 to the locked tube is equal to the difference in the tube axial load above and below TSP 6. The axial load below TSP 6 was determined in the previous paragraph. The loads are constant between the TSPs. At the time TSP 6 pressure is maximum, the axial load above TSP 6, which is equal to the axial load below TSP 7, is the sum of the contributions from pressure loading acting on TSP 7 as well as those transferred from the pressure loadings on the other TSPs. Positive values denote vertically upward forces transmitted from the TSP to the tube. As before, the maximum pullout loads do not necessarily occur at the same time. Note that large pullout forces act on the upper TSPs if only 1 or 2 tubes (per quarter TSP) are locked to the TSPs. The maximum pullout load is reduced to below 5 kips (21.4 KN) if 4 or more tubes (per quarter TSP) are locked to the TSPs.

Results for Slippage between TSPs and SG Tube When Maximum Tube Pullout Force Is Exceeded

The axial loads on the SG tube at the lower level will be reduced if the upper TSPs fail to transmit the full loads to the SG tube because of slippage. For example, if the maximum load that can be transmitted to the SG tube from a TSP is 5 kips (21.4 KN), the maximum axial load on the tube just below the 7th TSP will be reduced to 5 kips (21.4 KN). Figures 15a and b show the variations of maximum axial load and maximum forces transmitted from the TSP to the tubes when it is assumed that slippage occurs under a constant-load (5 kips [21.4 KN]) condition. Note that the axial loads are reduced significantly at the higher TSPs but not as much at the lower TSPs, because slippage between tube and TSP does not occur at the lower elevations. Similar plots for a pullout load of 1 kip (4.45 KN) are shown in Figs. 16a and b. In

this case, slippage occurs at all TSPs with numbers ≥3. The axial loads in all of the TSPs are reduced to ≤5 kips (21.4 KN).

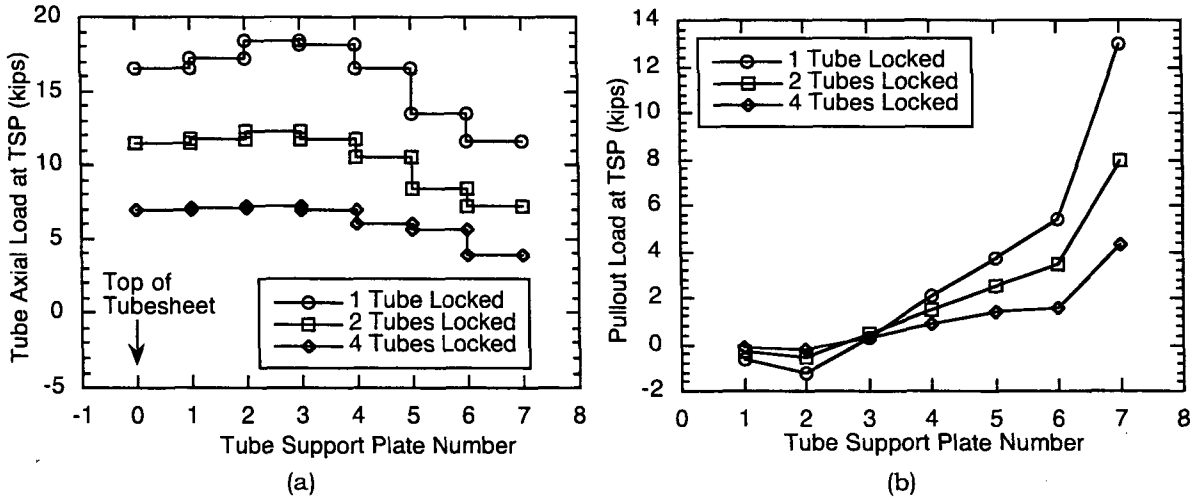

Figure 14. Variation of (a) maximum axial loads in SG tubes and (b) maximum loads transferred from TSPs to tubes at various TSP locations during large-break MSLB from hot standby. Note: 1 kip = 4.45 KN.

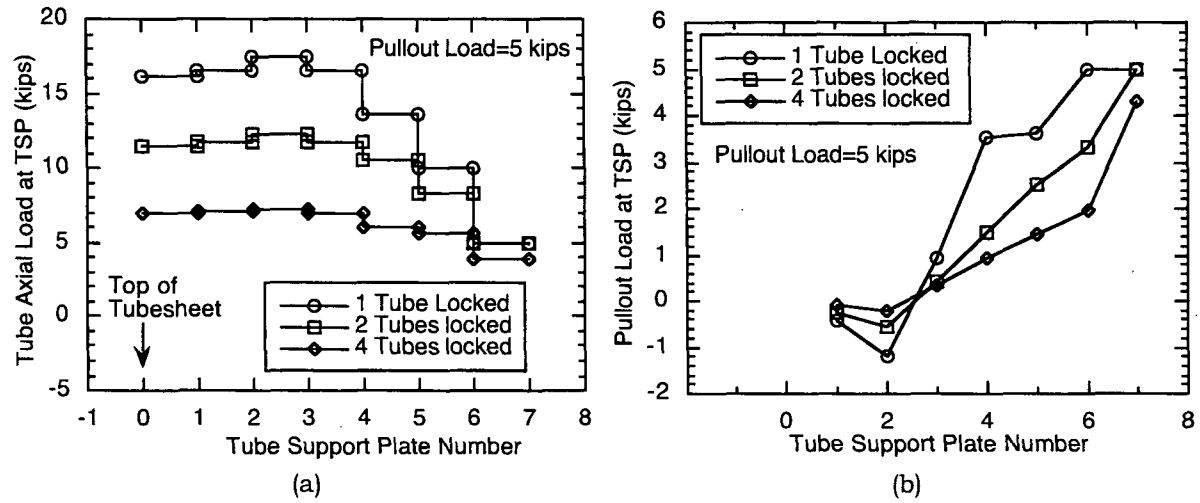

Figure 15. Variation of (a) maximum axial loads in SG tubes and (b) maximum loads transferred from TSPs to tubes at various TSP locations during large-break MSLB from hot standby, for tube pullout load of 5 kips (21.4 KN). Note: 1 kip = 4.45 KN.

4.3 Conclusions from Finite-Element Analyses

The transient dynamic analysis of the SG tube under transverse pressure loading shows that inertia effects should be negligible for the calculated rise time of the pressure pulse during a MSLB, and the maximum bending stress is small (<1 ksi [6.9 MPa]).

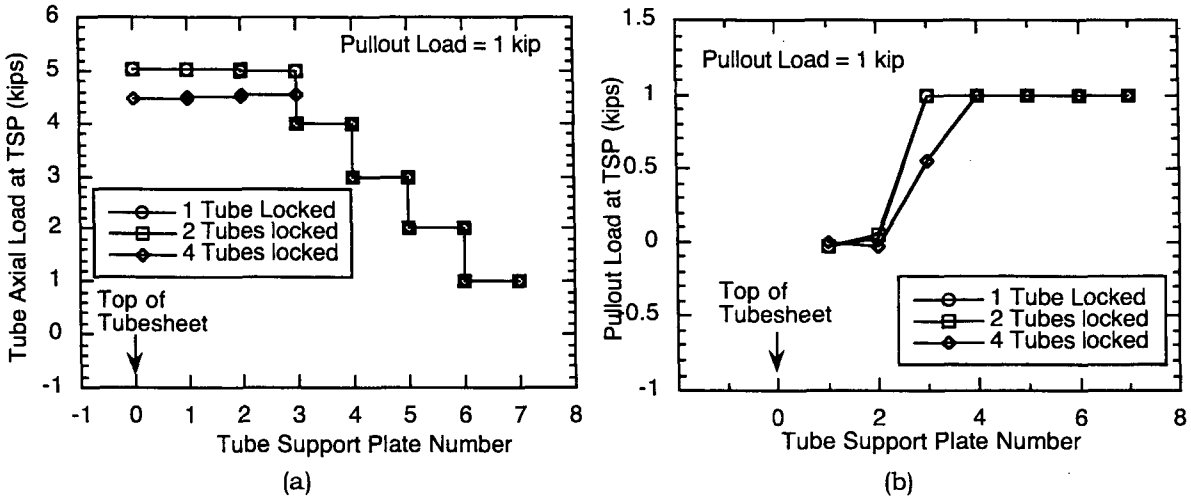

Figure 16. Variation of (a) maximum axial loads in SG tubes and (b) maximum loads transferred from TSPs to tubes at various TSP locations during large-break MSLB from hot standby, for tube pullout load of 1 kip (4.45 KN). Note: 1 kip = 4.45 KN.

The static FEA shows that the maximum displacement of the TSPs can be significantly reduced by the presence of a single locked tube. Maximum axial direct stresses dominate the maximum bending stresses in the tube. Thus, only axial loads transmitted to the tubes from the TSPs during the accident transients need be considered in the tube integrity calculations. Relatively large axial loads are created in the locked tube if no slippage occurs at the tube-to-TSP intersections. The upper TSPs transmit larger axial loads to the SG tubes because the pressure drops across the upper TSPs are larger than those across the lower TSPs. The transmitted loads are reduced if slippage at a constant load is allowed to occur at the tube-to-TSP junctions, and, the greater the reduction, the smaller the tube-to-TSP breakaway force. Although the pressure differentials across the lower TSPs are lower than those across the upper TSPs, significant fractions of the axial loads transferred to the locked tubes at the TSPs at higher elevation are transmitted undiminished as axial loads to the SG tubes at lower elevations. Because the magnitude of the tube axial loads depends critically on the maximum pullout loads at the tube-to-TSP junctions, we have reviewed the available tube pullout tests for Model 51 SGs in Section 5.

5 Review of Axial Pull Force Tests for Tube-To-TSP Intersections

Pull force data from laboratory pull force measurement tests, forces required to pull tubes from operating SGs (tubes initially cut above the TS with the TS section removed before force measurement), and tube/TSP/crevice deposit sections removed from the French Dampierre-1 SG have been summarized in Ref. 1. The data include measurements of the axial force necessary to displace a tube relative to the TSP for both dented and nondented TSP intersections. Most of the available data for pull forces is from nondented TSP intersections with tubes. The following sections on tube pull tests are based on the information provided in Ref. 1.

5.1 Laboratory Pull Force Tests

Laboratory tests were performed to assess the effects of denting and packed crevices on the forces required to displace a tube relative to the TSP.[1] The specimens were first fatigue cracked to throughwall (TW) lengths of 0.3-0.7 in. (7.62-17.8 mm), and then dented in the laboratory to obtain dent voltages between 0 and 17.4 volts. Pull force tests were performed on 7 specimens. The results are summarized in Table 6. The results show that forces of 80-700 lbs (356-3114 N) were required to displace the TSP for dents ≤5 volts. The highest force of 700 lbs (3114 N) was obtained for a specimen with no measurable dent voltage. With dent voltages between 6 and 12 volts, pull forces ranged from 3220 to 4200 lbs (14323 to 18682 N).

Table 6. Summary of laboratory pull force test results for dented TSP intersections

Specimen	Dent Volt	TW Crack Length, in. (mm)	TSP Pull Force, lbs (KN)
FAT-2	6.1	0.3 (7.62)	4200 (18.7)
FAT-3	12.1	0.3 (7.62)	3220 (14.3)
FAT-5	4.6	0.3 (7.62)	475 (2.11)
FAT-6	0	0.3 (7.62)	700 (3.11)
FAT-9	3.4	0.5 (12.5)	85 (0.38)
FAT-10	2.5	0.7 (17.8)	85 (0.38)
FAT-11	2.8	0.5 (12.5)	80 (0.36)

5.2 Pulled-Tube Force Measurements

Pulled-tube force measurements can be used to estimate forces required for TSP displacement when the tube section being pulled includes only tubing above the top of the TS. In the field most tube pulls are performed by cutting the tube at the desired elevation and pulling it through the TS. This type of tube pull includes the drag on the tube due to friction within the TS and the associated pull forces must be used with caution when estimating the forces for TSP displacements. Another difference between tube pulls and the behavior of the tubes during an accident also must be considered. During tube pulls, the Poisson's contraction of the tube diameter will tend to lower the friction forces within the TSP. On the

other hand, an increase in the pressure differential across the tube wall during a MSLB event will increase the tube diameter, leading to an increase in frictional forces.

5.2.1 Plant L Pulled Tube

The tube pull forces for Plant L were obtained by first cutting the tube above the top of the TS, removing the tube within the TS, drilling a slightly larger TS hole and then pulling the tube section above the TS. With this method, the initial pull force on the tube section above the TS represents the breakaway force for displacing the tube relative to the TSPs. No denting was detected at the TSP intersection for the pulled tube from this unit. The initial force needed to move the tube represents the breakaway force of the 3 pulled TSP intersections. The measured breakaway forces for Plant L are:

R29C70	7955 lbs (35.4 KN) breakaway	≈2650 lbs (11.8 KN) per intersection
R18C70	4955 lbs (22.0 KN) breakaway	≈1650 lbs (7.3 KN) per intersection
R30C64	2775 lbs (12.3 KN) breakaway	≈925 lbs (4.1 KN) per intersection.

The above breakaway forces of 925-2650 lbs (4.1-11.8 KN) per intersection measured in the field for tubes with no denting are higher than the value of 700 lbs (3.1 KN), measured in the laboratory for a tube with incipient denting.

5.2.2 Plant G-1 Pulled Tube

In Plant G-1, a standard method, in which the diameter of the tube within the TS was reduced by melting some of the tube material with a weld torch, was used to remove a tube section. As the tube was pulled into the channel head, segments, typically 2-3 ft (0.6-0.9 m) long, were cut off and removed. A portion of the tube from Plant G-1 included all of the intersections up to the top TSP. The actual sever of the tube was at the top of the top TSP. For the first 4 feet of tube motion, the pull force was of the order of 9700 lbs (43 KN), which corresponded to motion through six TSPs. A step reduction in the pulling force occurred; it corresponded to the end of the tube passing through the TSP that was next to the top. For the next 4 feet, the pull force was 6300 lbs (28 KN), which corresponded to motion through five TSPs. Another step change in pull force was noted when the end of the tube passed through the next TSP, leading to a load of ≈4500 lbs (20 KN), which corresponded to motion through 4 TSPs. Although the pull force measurements include drag through the TS, the drop in forces after the tube passes through a TSP is a measure of the tube-to-TSP contact force. Thus, the pull force measurements imply pull forces through dented TSPs of 3400 lbs (15 KN) and 1800 lbs (8 KN) after more than 8 ft (2.44 m) of tube moved through the TSPs. The top TSP contained a dent of ≈0.012 in. (0.30 mm), as measured by profilometry, and smaller dents were present in the lower TSPs.

5.2.3 Pull Force Measurements on Tubes Removed from Dampierre-1

The sections removed from a replaced Dampierre-1 SG included the tube, TSP, and the crevice deposits, which retained the tube in the TSP during the removal operation. Electricitè de France (EdF) does not consider Dampierre SGs particularly dirty in terms of sediments or

corrosion, and they consider the crevice deposits to be typical of SGs with drilled carbon steel TSPs. On some tubes, tube pullout forces were measured without chemical cleaning, and on other sections, after chemical cleaning. Thus, the data provide information on the effect of chemical cleaning on tube-to-TSP forces. Dampierre-1 commenced operation in 1980 and the SGs were replaced in 1990.

Table 7. Axial force required to displace tubes relative to TSP for tubes removed from Dampierre-1 and not chemically cleaned

TSP No.	Test Temp., °F (°C)	TSP disp., in. (mm)	Force, lbs (KN)	Average Force, lbs (KN)
8	70 (20)	0.08 (2.0)	1310 (5.8) 2460 (10.9) 2640 (11.7) 3470 (15.4)	2600 (11.6)
7	70 (20)	0.12 (3.0)	3103 (13.8) 4496 (20.0) 2181 (9.7)	3338 (14.8)
7 8	70 (20)	0.16 (4.1)	2563 (11.4) 3822 (17.0) 4339 (19.3) 1686 (7.50)	3102 (13.8)
8 7	70 (20)	0.20 (5.1)	2644 (11.8) 2600 (11.6) 2823 (12.6) 3093 (13.8) 3192 (14.2) 2922 (13.0) 3754 (16.7) 4137 (18.4)	3145 (14.0)
8	70 (20)	0.39 (9.9)	3453 (15.4) 3759 (16.7) 3363 (15.0) 3111 (13.8)	3421 (15.2)
8	547 (286)	0.08 (2.0)	3260 (14.5) 3664 (16.3) 1800 (8.0) 2070 (9.2)	2700 (12.0)
8	547 (286)	0.20 (5.1)	3192 (14.2) 3664 (16.3) 1619 (7.2) 2360 (10.5)	2709 (12.0)
8	547 (286)	0.39 (9.9)	2922 (13.0) 3777 (16.8) 1641 (7.3) 2270 (10.1)	2653 (11.8)

Data on axial forces for TSP displacements from Dampierre-1 are listed in Table 7 for specimens without chemical cleaning (at room temperature [RT] and 547°F [286°C]) and, in Table 8, for specimens with chemical cleaning at RT. Note that the TSP forces are approximately independent of TSP displacement for TSP displacements between 0.08 in (2.0 mm) and 0.2 in. (5.1 mm). The overall average forces needed to displace the TSP relative to the tube are 3120 and 2686 lbs (13.9 and 11.9 KN) at 70°F (20°C) and 547°F (286°C), respectively, for tubes without chemical cleaning. After chemical cleaning, the overall average force to displace the TSP relative to the tube at 70°F (20°C) drops to 1559 lbs (6.9 KN), which is an ≈50% reduction from that without chemical cleaning.

Table 8. Axial force required at room temperature to displace tube relative to TSP in tubes removed from Dampierre-1 and chemically cleaned.

TSP No.	TSP Disp., in. (mm)	Force, lbs (KN)	Average Force, lbs (KN)
1	0.12 (3.0)	1574 (7.0)	1574 (7.0)
1	0.16 (4.1)	1012 (4.5) 2023 (9.0) 1799 (8.0) 2091 (9.3)	1731 (7.7)
1	0.20 (5.1)	1259 (5.6) 1371 (6.1) 1057 (4.7) 1844 (8.2)	1383 (6.2)

Table 9. Summary of axial forces in lbs (KN) required to displace tube relative to TSP of a replaced Dampierre-1 SG at room temperature and 547°F (286°C).

Parameter	Without chemical cleaning		With chemical cleaning	
	70°F (20°C)	547°F (286°C)	70°F (20°C)	547°F (286°C)
Mean Force	3120 (13.9)	2686 (11.9)	1559 (6.9)	1342 (6.0)[a]
No. of tests	23	12	9	0
Standard deviation	792 (3.5)	821 (3.7)	405 (1.8)	405 (1.8)[a]
Upper 95% confidence	4427 (19.7)	4041 (18.0)	2227 (9.9)	2010 (8.9)
Lower 95% confidence	1813 (8.1)	1331 (5.9)	891 (4.0)	674 (3.0)
Minimum measured	1310 (5.8)	1619 (7.2)	1012 (4.5)	-
Maximum measured	4496 (20.0)	3770 (16.8)	2091 (9.3)	-

[a] Operating pull forces based on applying 0.86 ratio of operating to RT, obtained from tests without chemical cleaning and assuming same standard deviation as RT result

The results for Dampierre-1 tests on axial forces needed to displace the TSP relative to the tube for nondented tubes removed from a replaced SG are summarized in Table 9. Included in the table are mean, standard deviation, and upper and lower 95% confidence values. We have used 4000 lbs (17.8 KN) as an upper bound and 2700 lbs (12.0 KN) as the average axial load transmitted from a TSP to a locked tube at 547°F (286°C) for tube integrity calculations.

6 Effect of MSLB on Flawed Tubes

The FEA results in Section 4 showed that loads transferred from TSPs to locked SG tubes during a large-break MSLB event are important for determining the stresses in locked tubes and that the loads transmitted from the TSPs to the locked tubes are primarily axial. In this section, we consider the effect of such an axial load on the stability of both axial and circumferential cracks. The material properties used for all calculations in this section correspond to those of an average Alloy 600 tube and are as follows:

RT yield stress = 43 ksi (296 MPa)

RT ultimate tensile strength = 98 ksi (676 MPa)

The properties are reduced by 8% at 550°F (286°C).

For reference, ≈5.1 kips (22.7 KN) of axial load are required to cause yielding and 11.7 kips (52 KN) axial load is required to cause failure of an unflawed 7/8-in. (22.2-mm)-diameter SG tube at 550°F (286°C).

6.1 Axial Cracks

It is generally felt that axial tensile loads transmitted to the SG tubes by the TSP during a SLB event should not significantly affect the burst pressure and leak rate characteristics of SG tubes with axial cracks. However, few experimental results or analyses are reported on this topic in the literature.

6.1.1 0.5-in. Throughwall Axial Crack

Finite-deformation elastic-plastic analyses of a SG tube with a 0.5-in. (13-mm)-long midspan TW axial crack were carried out for 2 cases both of which involved an applied internal pressure (p) and an end cap axial load ($p\pi R^2$) increasing proportionally from zero to a maximum. In both cases the maximum internal pressure was 5 ksi (34.5 MPa) and the tube was a 0.875-in. (22.2 mm)-OD Alloy 600 SG tube. In the first case, which simulated a free-to-slide boundary condition at the TSP, the maximum axial load was 2400 lbs (10.7 KN). In the second case, which simulated a SG tube locked at the TSP, the maximum axial load was 5000 lbs (22.2 KN)

Figure 17 shows a plot of the calculated opening displacement (or stretch) of the crack tip as a function of pressure for both boundary conditions. As expected, the crack tip opening displacement (CTOD) is decreased slightly by the application of the axial load. Assuming that unstable burst occurs at a CTOD equal to the tube wall thickness, the burst pressure increases from ≈4.3 ksi (29.6 MPa) (free to slide) to 4.4 ksi (30.3 MPa) (locked TSP). Note that tests at Argonne National Laboratory (ANL) show that the burst pressure of a 7/8-in. (22.2-mm)-diameter tube with a 0.5-in (13-mm) TW crack varies between 3.8 and 4.8 ksi (26 and 33 MPa).[5]

The shapes of the crack opening displacement (COD) and radial bulging displacement curves at a pressure of 2.5 ksi (17 MPa) (representing SLB pressure conditions) are shown in Figs. 18a and b, respectively. The decreases in COD and crack opening area (COA) going from a free-to-slide to the assumed locked-TSP loading condition are ≈10%. The change in the bulging displacements are even less.

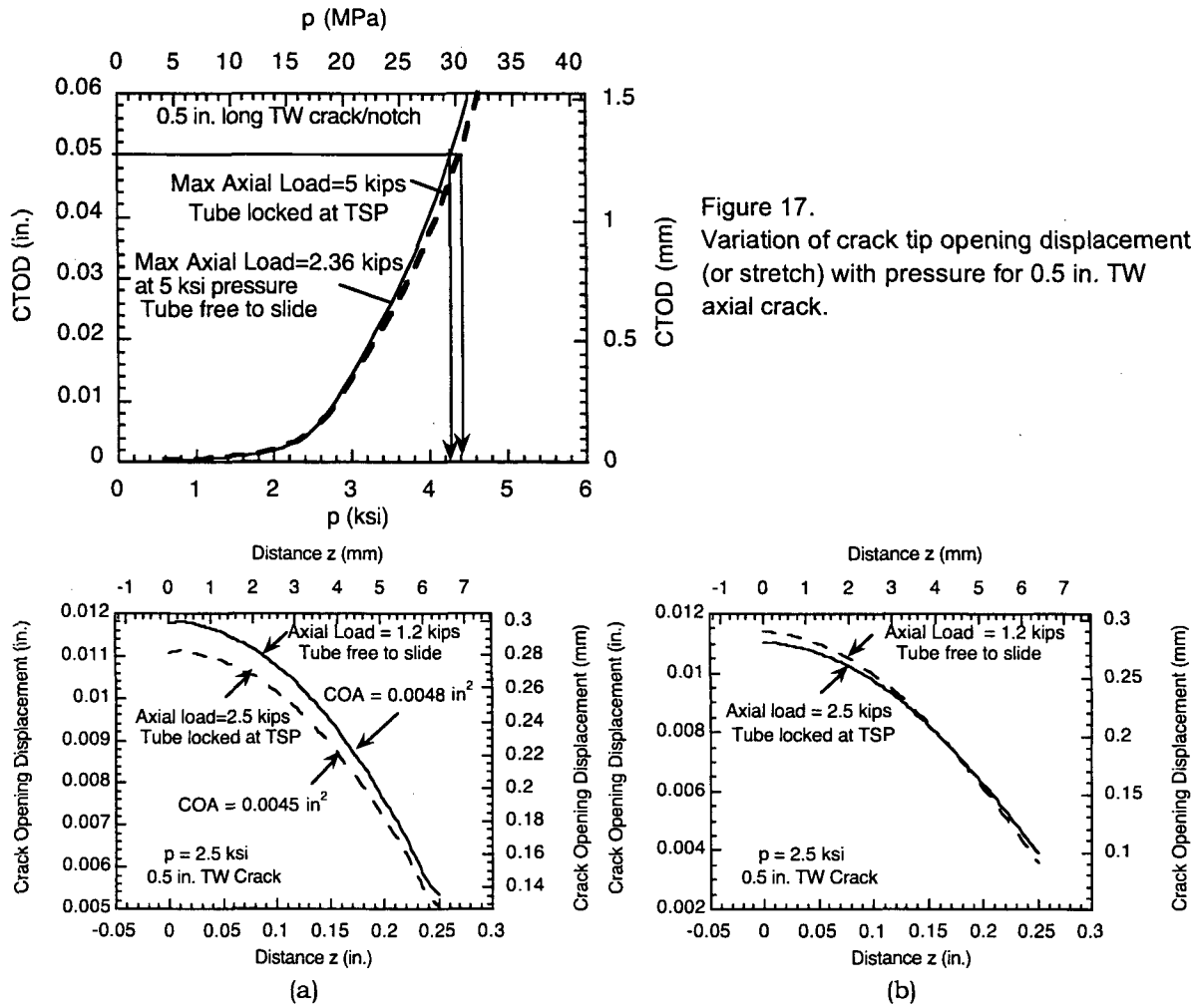

Figure 17.
Variation of crack tip opening displacement (or stretch) with pressure for 0.5 in. TW axial crack.

Figure 18. (a) Shape of COD and (b) radial bulging displacement for a 0.5-in. (13-mm) TW crack at pressure of 2.5 ksi (17 MPa) for 2 axial boundary conditions. Note: 1 kip = 4.448 KN.

6.1.2 0.25-in. (6-mm) TW Axial Crack

Similar analyses were conducted for a 0.25-in. (6-mm)-long crack. However, the analysis failed to converge beyond a pressure of 5.6 ksi (38.6 MPa) if the crack width was taken as zero (Fig. 19). To eliminate the convergence problem, the model was modified to represent an 8-mil (0.2-mm)-wide electrodischarged machined (EDM) notch. Figure 19 shows a plot of the calculated notch tip opening displacement (or stretch) of the crack as a function of pressure for both boundary conditions. Note that the notch results are close to the crack results. In contrast to the results presented for the longer 0.5-in. (13-mm) TW crack in Section 6.1.1, the

CTOD is almost unchanged when the boundary condition is changed from free-to-slide (solid line) to locked (bold dashed line) at a TSP with an applied axial tensile load of 5000 lbs (22.2 KN). Assuming that unstable burst occurs at a CTOD equal to the tube wall thickness, the burst pressure for both free-to-slide and locked-tube conditions is 6.7 ksi (46 MPa). ANL tests show that the burst pressure of a 7/8-in.(22.2-mm)-diameter tube with a 0.25-in. (6-mm) TW EDM notch varies between 6 and 7 ksi (41 and 48 MPa), consistent with the calculated results that use the CTOD failure criterion.[5]

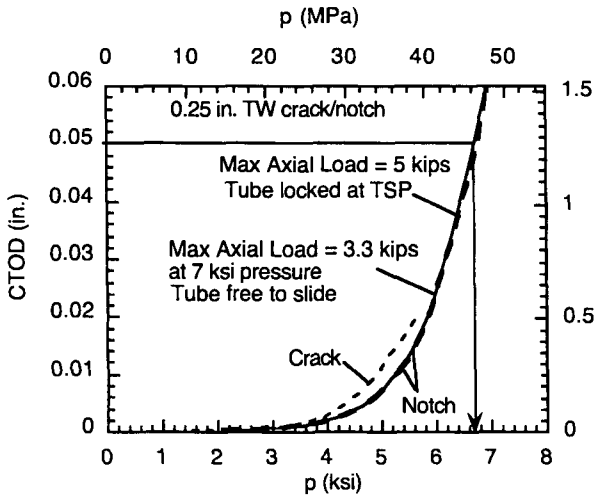

Figure 19.
Variation of crack and notch tip opening displacement (or stretch) with pressure for 0.25-in. (6-mm)-long TW axial crack and EDM notch. Note: 1 ksi = 6.8 MPa and 1 kip = 4.448 KN.

6.1.3 Conclusions for Axial Cracks

Axial loads up to 5000 lbs (22.2 KN) applied to a SG tube do not significantly change the burst pressure or crack opening characteristics of cracks that are ≤0.5 in. (13 mm). The influence of the axial load on burst pressure or crack opening decreases with decreasing crack length.

6.2 Circumferential Cracks

In this section, we investigate the effect of an axial load due to a locked TSP on the crack driving force of a TW circumferential crack at the top of a TS or TSP at 550°F (286°C). Two models are available for computing the crack driving force J (or K_J) for this loading and crack configuration. The first is Zahoor's model,[6] which assumes that the SG tube is free to bend (Fig. 20a). The other is an ANL model,[5] which is based on a rigid-plastic material model and assumes that the ligament is at incipient collapse (Fig. 20b). Zahoor's model is independent of the unsupported span between the TS and the first TSP. The ANL model accounts for the constraining effect of the TSP; therefore, its results depend on the unsupported span length. An infinitely long unsupported span would correspond to a free-to-bend boundary condition. The free-to-bend assumption of Zahoor's model gives acceptable results at low axial loads, but at higher loads, the restraining effect of the TSP can significantly reduce the crack driving force.

Figures 21a and b show the variations of the crack driving force K_J with axial load when the Zahoor and ANL models are used for 2 unsupported spans of a SG tube with a 135° and 180° TW circumferential crack, respectively. Note that by choosing a sufficiently large unsupported span, the results from the ANL model can be made to agree with Zahoor's model. The ANL model does not register a large crack driving force until the ligament reaches collapse (rigid-plastic). However, the ANL model predicts that an unsupported span of 50 in. (1.3 m) can lead to a significant reduction of crack driving force, when compared with the free-to-bend case, at higher axial loads.

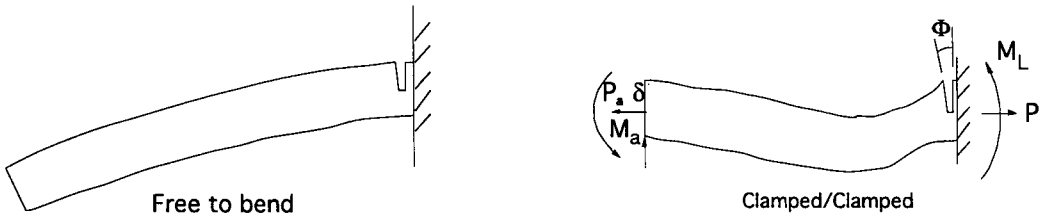

(a) (b)

Figure 20. Free-to-bend (Zahoor model) and clamped/clamped (ANL model) deformation modes of a SG tube with a TW circumferential crack under axial loading.

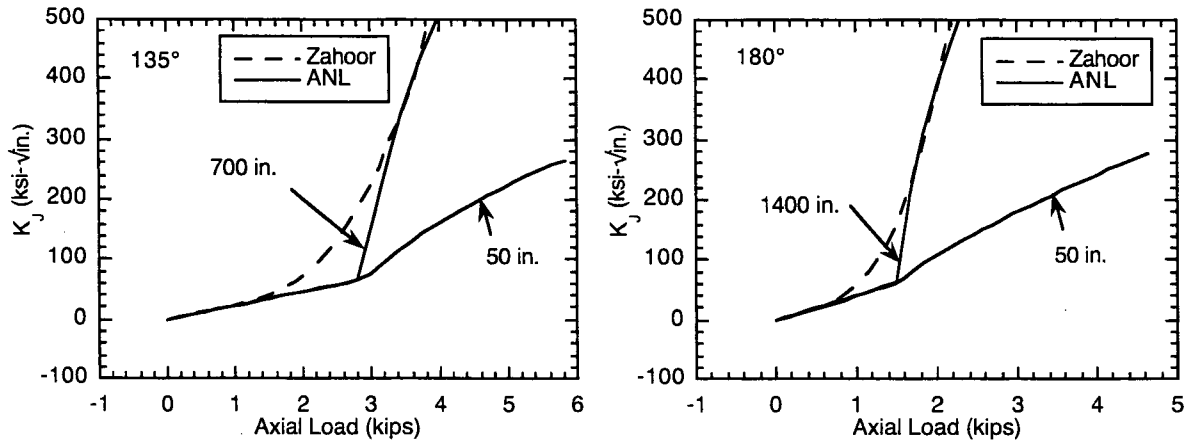

(a) (b)

Figure 21. Crack driving force K_J for (a) 135° (with 50- and 700-in. (1.3- and 18-m) unsupported span) and (b) 180° (with 50- and 1400-in. [1.3- and 36-m] unsupported span) circumferential TW crack as functions of axial load. Note: 1 ksi√in = 1.1 MPa√m and 1 kip = 4.45 KN.

6.2.1 All Tubes Locked at All TSPs

The analysis of this case for a Model 51 SG was summarized in Section 3 and the results showed that the maximum axial load per tube during a large-break MSLB was 1.6 kips. Using 50 in. (1.3 m) as a typical span between TSPs of a Model 51 SG, in Fig.22, we plotted the failure axial load of a 7/8-in.(22.2-mm)-diameter SG tube at 550°F (286°C) as a function of TW crack angle. The longest TW circumferential crack that can be tolerated for an axial load of 1.6 kips (7.1 KN) is ≈300°.

6.2.2 Single Tube Locked at 1 TSP Intersection

If we use 4 kips (17.8 KN) as an upper bound to the TSP locking force (see Section 5.2.3) for a SG tube, and allow 1.2 kips (5.3 KN) as the additional axial load due to end-cap effects (pR/2t) due to MSLB pressure of 2.5 ksi (17 MPa), the maximum permissible TW crack angle is 160°. At an average TSP locking force of 2.7 kips (12 KN), the maximum permissible TW crack is 210°.

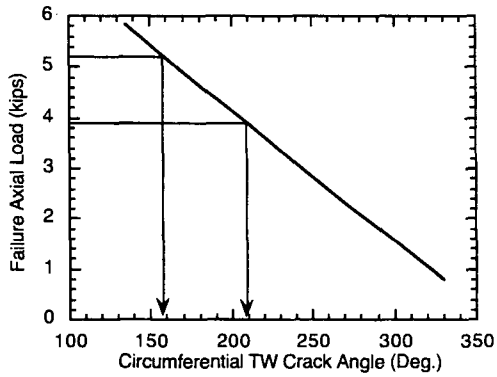

Figure 22.
Failure axial load vs. circumferen-tial TW crack length for a 7/8-in.-diam SG tube with 50-in. unsupported span. Note: 1 kip = 4.45 KN.

6.2.3 1 or More Tubes Locked at All TSP Intersections

The worst case, from the viewpoint of tube integrity, occurs when a single tube is locked at all TSPs, and all of the other tubes are free to slide. As noted previously in Section 4.2.1, this is highly unlikely to occur in practice. Experience suggests that a large fraction of the tubes are likely to be able to withstand significant pullout forces. However, as "worst" case analyses, solutions for 1, 2, 4, and 10 tubes locked at all of the TSPs were considered. A plot of the maximum values of the tube axial load at all of the TSPs, corresponding to the pressure data given in Fig. 1a (multiplied by the uncertainty factor of 1.5), when 1, 2, 4, and 10 tubes are locked to all of the TSPs in a local region, is given in Fig. 23a for the case where the maximum locking force is 4 kips (17.8 KN) per tube per TSP junction (upper bound value from Section 5.2.3). A similar plot for the case where the maximum locking force is the average value of 2.7 kips (12 KN) per tube per TSP junction is given in Fig. 23b. Note that the distribution of axial loads in the locked tubes becomes more uniform as the number of locked tubes is increased. The loads transferred from the various TSPs to the tubes for these 2 cases are plotted in Figs. 24a and b. A negative pullout load signifies load transferred from the TSP to the tube in the vertically downward direction. Note that, if 10 tubes are locked, no slippage is predicted at any of the TSP intersections.

If only 1 or 2 tubes are locked to all of the TSPs while the rest are free to slide, the maximum axial stresses in the locked tubes at mid to lower elevations are close to the ultimate tensile strength. Despite the large values calculated for the stresses, it cannot be concluded that unflawed tubes would actually fail, because large plastic displacements are required before rupture can occur. These large stresses, however, do significantly reduce the size of circumferential crack that can be tolerated.

The maximum allowable size for circumferential TW cracks at the top of the TS and TSPs for the cases with 4 and 10 locked tubes and with tube pullout force of 2.7 (average) and 4 kips (upper bound) (12.0 [average] and 17.8 KN [upper bound]) are given in Fig. 25. These calculations include the additive axial load on the tubes due to MSLB pressure acting on the U-bend end cap.

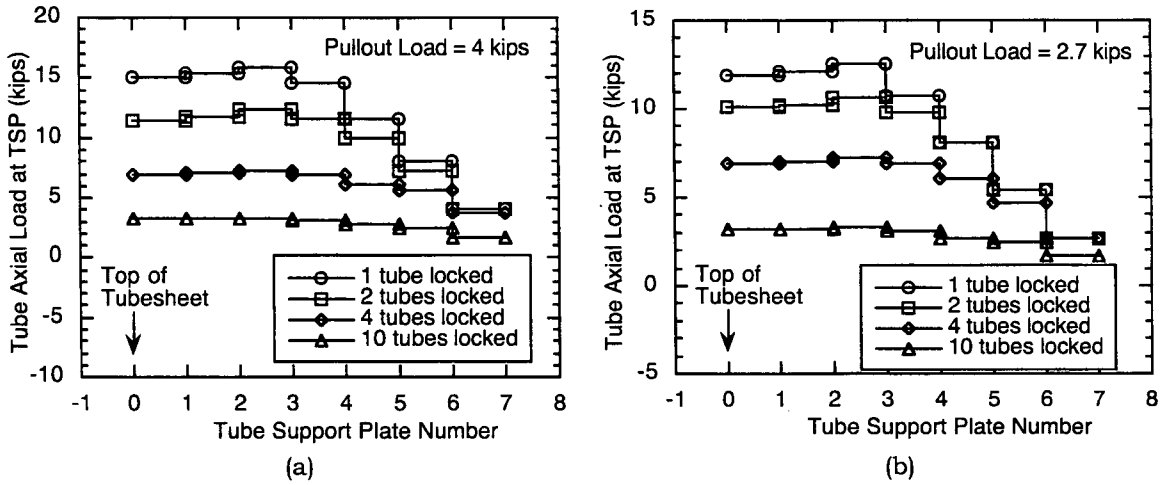

Figure 23. Maximum axial tube load at various TSPs during large-break MSLB with 1, 2, 4, and 10 tubes locked, for TSP pullout loads of (a) 4 kips and (b) 2.7 kips. Note: 1 kip = 4.45 KN.

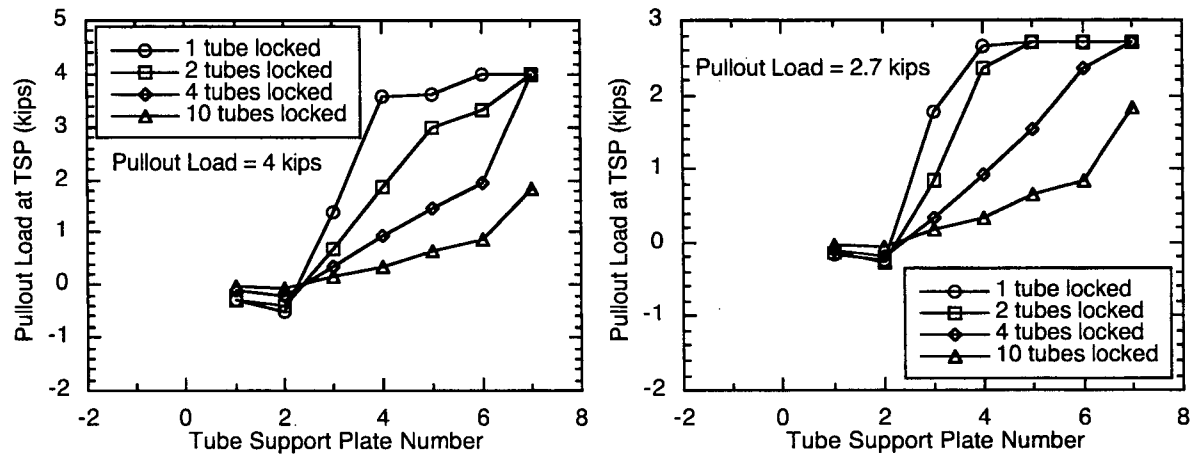

Figure 24. Variation of maximum loads transferred from TSPs to tubes at various TSP locations during large-break MSLB from hot standby, for tube pullout load of (a) 4 kips and (b) 2.7 kips. Note: 1 kip = 4.45 KN.

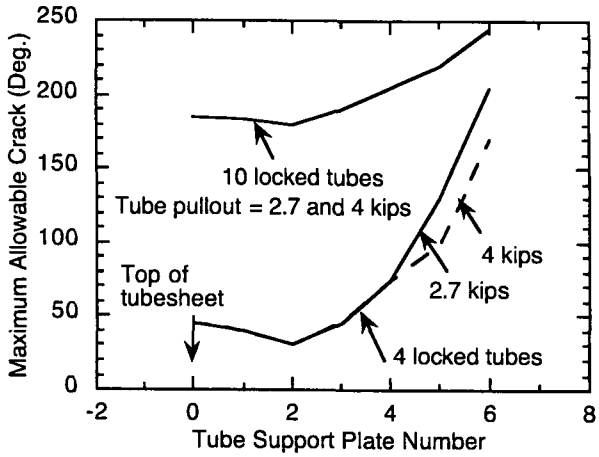

Figure 25.
Maximum allowable TW cracks at top of TS and TSPs for 4 and 10 locked tubes with 2.7- and 4-kip tube pullout loads. Note: 1 kip = 4.45 KN.

7 Crack Growth Analysis

In the previous Section, we considered the case of rupture of SG tubes that contain circumferential TW cracks by a 1-time application of a load. In this Section, we consider the potential for such cracks to grow by repeated application of the load during a MSLB. Although TH analyses to date show, at most, 1 or 2 cycles of pressure pulses (Fig. 1), we carried out the fatigue analysis to estimate the available margin against failure if the MSLB pressure cycles were to be applied repeatedly. Environmental effects will be unimportant for the frequencies of interest.

To analyze fatigue crack growth, we used the following correlation (load ratio R = 0) for Alloy 600 at 550°F in an air environment

$$\frac{da}{dN} = 3.43X10^{-12}\Delta K^{3.3}. \quad (2)$$

This correlation, given in the current ASME Code Section XI, is based on the work carried out by James and Jones.[7] In Eq.2, da/dN is the crack growth per cycle (m/cycle) and ΔK is the stress intensity factor range (in MPa-$m^{1/2}$). To be conservative, no threshold stress intensity factor was assumed. We calculated the stress intensity factor range ΔK_J from the J correlation of Zahoor[6] for part-throughwall (PTW) circumferential cracks and from ANL[5] for TW circumferential cracks with a span of 50 in. (1.3 m), using the following equation:

$$\Delta K_J = \sqrt{E\,\Delta J}, \quad (3)$$

where E is the Young's modulus. For PTW cracks, we first considered crack growth in the depth direction until the crack became TW and then we considered the growth of the TW crack in the circumferential direction until rupture was predicted. Rupture was predicted to occur when either the uncracked section that contained the crack reached a plastic collapse state or a maximum K_J value of 300 ksi-$\sqrt{in}$ (330 MPa-$\sqrt{m}$) was attained. In most cases, the former criterion controlled the final rupture.

7.1 Initially Throughwall Cracks

Figure 26a shows the calculated cycles to failure as a function of initial TW crack length for various axial loads. From Fig. 23a, we note that the axial loads at the various TSP elevations vary from 4 to 7 kips for the case when 4 tubes are locked and from 2 to 3 kips (8.9 to 13.3 KN) when 10 tubes are locked. Note that the curves become relatively flat when the number of cycles to failure is small. Thus, at 7-kips (31-KN) axial loading, 30 cycles are required to grow the crack from 85° to final instability at 87°, but 150 cycles are required to grow the crack from 80 to 87°. At 4 kips (17.8 KN), 90 cycles are required to grow the crack from 195° to the instability length of 205°. At 3 kips (13.3 KN), 95 cycles are required to grow the crack from 230° to the instability length of 240°. At 2 kips (8.9 KN), 100 cycles are required to grow the crack from 270° to the instability length of 280°. Thus, in all cases, the crack growth rates during the cycles immediately before instability are quite slow (~0.1° per cycle).

7.2 Initially Part-Throughwall Cracks

To illustrate the effect of PTW cracks, in Fig. 26b, we present the cycles to failure for initially 80% PTW cracks with those for 100% TW cracks in 2 load ranges. The figure indicates that the additional cycles needed to grow the initially PTW crack through the wall thickness of the tube add significant margins at the low-cycle end, where the curves, instead of becoming flat (horizontal), turn upward, so much longer initial cracks can be tolerated at the same cycles to failure.

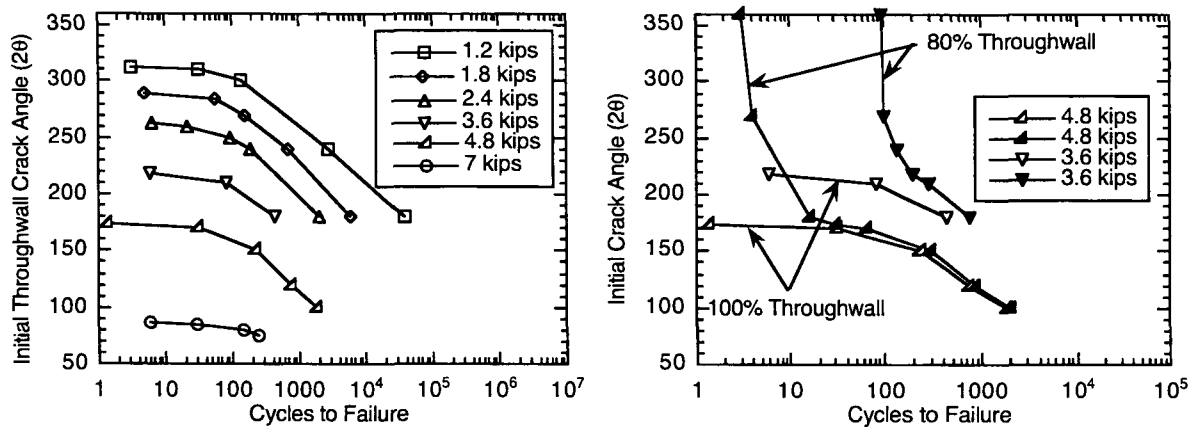

Figure 26. Cycles to failure vs. initial crack angle for (a) TW and (b) PTW circumferential cracks for various zero-to-maximum axial loading. Note: 1 kip = 4.45 KN.

8 Discussion and Conclusions

A review of the available TH analyses of MSLB and FWLB for the Westinghouse Model 51 and Model E2 SGs showed that the most critical transient, from a SG tube integrity standpoint, is the large-break MSLB event. During such an event, the pressure drops across the TSPs are the highest, and they increase with increasing TSP elevation. The lateral pressure load on the tubes is also highest during a large-break MSLB, but the pressures are too low to cause significant bending stress (<1 ksi) in the tubes. It was shown that the periods of the fundamental vibration modes of the tubes and the TSPs are sufficiently short when compared with the rise time of the pressure pulse during a MSLB so inertia effects may be ignored.

Static-elastic FEAs of a Model 51 SG TSP, including the supports, and with and without a single tube (at the maximum displacement point) locked to the TSP, showed that the maximum TSP displacement under a unit pressure loading is reduced from 0.44 to 0.054 in. (11 to 1.4 mm), whereas the displacement of the TSP at the tube-to-TSP junction (which had been the maximum displacement point) is reduced to 0.013 in. (0.3 mm). These results are in agreement with industry reports,[1,2] which show that the axial stiffness of the SG tubes is far greater than the bending stiffness of the TSPs, whose stiffness is reduced significantly because of the presence of numerous tube and flow holes.

The analysis in Ref. 1 assumed that all of the tubes were locked into the TSPs. A comparison of the resultant loads transferred from the plates to the tubes showed that they are relatively small when compared with the pullout forces measured on actual SGs.

To assess the "worst case" situations, when only a small number of tubes are locked, a simplified but conservative finite-element model of the 7 TSPs of a Model 51 SG, including the supporting stay rods and wedges, was developed. The supporting rods and wedges were assumed to provide rigid support to the TSPs. Interaction between the TSPs was modeled by the locked SG tubes only. The tubes were assumed to be fixed to the TS, which was assumed to be rigid. Approximate analyses were carried out with 1, 2, 4, and 10 tubes in a local region locked to the TSPs. Unit pressure drop (upward) analysis for each of the TSPs in turn showed that the pressure load was primarily transferred as tensile axial load on the locked SG tubes below the loaded TSP, although ≈10-15% of the load was carried as axial compressive load in the tube sections above the loaded TSP. The axial load per tube decreased steadily as the number of locked tubes was increased, as expected. Also, the results showed that the maximum bending stress in the tubes is much smaller than the maximum direct axial stress. Therefore, the tube integrity calculations were conducted for tubes under axial loading only.

The results of unit pressure drop analysis were used to calculate the axial loads acting on the various tube sections of the Model 51 SG under a large-break MSLB transient pressure drop loading on the TSPs. The pressure drops associated with MSLB reported in Refs. 1 and 2 were compared with calculations performed with the NRC TH code, TRAC-M and reported in a NRC report by Krotiuk.[4] There is generally good agreement between the various calculations. For the present calculations, we used the results of Krotiuk.[4] The reported pressure drops were multiplied by an uncertainty factor of 1.5, as suggested by the author. In the case where only a few tubes are locked, initial analysis results showed that unrealistically large loads

were transferred from the TSPs to the locked SG tubes if no consideration was given to the maximum pullout load capability of the tube-to-TSP joint. A review of tube pullout data from a retired SG from Dampierre (summarized in Ref. 1) showed that the mean value of the tube pullout load at operating temperature is 2.7 kips (12 KN) per tube per intersection and a reasonable upper bound (upper 95% confidence limit) is 4 kips (17.8 KN) per tube per intersection.

Reanalyses showed that, even when the maximum tube pullout capability was limited to more realistic values, the calculated axial tensile stresses on the locked tubes at lower elevations exceeded the ultimate tensile strength if only 1 or 2 tubes were assumed to be locked at the TSPs. Although this finding by itself would not suggest rupture of the locked tubes if they were unflawed, it would imply that tolerance for circumferential cracks in these tubes could be severely limited. The loads transferred to the SG tubes during the transients have virtually no effect on the burst pressure and leak rate integrity of tubes with axial cracks.

If the number of locked tubes in each region is increased to 10, the maximum axial load in the locked tubes is reduced to 3 kips and the allowable TW circumferential cracks in the tubes at all of the TSP junctions would be ≥180°. If all tubes are locked to all TSPs, the maximum tube axial load is 1.6 kips (7.1 KN) and the permissible crack length is ≥300°.

Although the available TH results for the MSLB transient show at most 1 or 2 pressure pulse peaks, fatigue analyses were conducted to demonstrate that sufficient margin exists for crack growth in the event that the pressure drop pulses were to occur repeatedly. The fatigue analysis showed that the average crack growth rate for 100% TW circumferential cracks, just before rupture, is of the order of only 0.1°/cycle. With as few as 16 tubes locked (4 tubes/region), circumferential TW cracks ≤85° would not grow to failure. With 40 tubes locked (10 tubes/region), cracks ≤230° would not grow to failure. If the cracks are PTW, longer cracks can be tolerated.

The results of the present study show that if even a few percent of the tubes in a SG are locked to the TSPs by crevice deposits or corrosion products, the dynamic loads associated with MSLB will have little impact on the integrity of SG tubes unless extensive circumferential cracking is present. Anecdotal evidence and the results of the extensive study on the pullout forces at Dampierre strongly support the conclusion that SGs with drilled hole carbon steel tube support plates will have enough tubes locked that the dynamic loads will be of little concern. Although there is limited pullout force data, measured values from US steam generators are comparable to those in Dampierre.

As noted previously, industry calculations of pressure drops across the TSPs due to a MSLB with RELAP5, and NRC staff calculations with TRAC-M, give comparable results. In addition, both the industry and the staff have undertaken bounding analyses of the pressure drops that give comparable results and are about a factor of 2 higher than the code calculations. Therefore, no additional TH analysis is necessary.

References

1. Model 51 Steam Generator Limited Tube Support Plate Displacement Analysis for Dented or Packed Tube-to-Tube Support Plate Crevices, WCAP-14707, Westinghouse Electric Corporation, August 1996. *Proprietary information. Not publicly available.*

2. Technical Support for Implementing High-Voltage Alternate Repair Criteria at Hot Leg Limited Displacement TSP Intersections for South Texas Plant Unit 2, Model E Steam Generator, WCAP-15163 Revision 1, Westinghouse Electric Corporation, March 1999. Also, WCAP-15163 Addendum Revision 1, January 2001. *Proprietary information. Not publicly available.*

3. V. Bhasin et al., "Structural Analysis of Steam Generator Internals Following Feed-Water/Main-Steam-Line Break: DLF Approach," BARC/1993/E-026, Bhaba Atomic Research Center, Bombay, India, 1993.

4. W. J. Krotiuk, "Pressurized Water Reactor Steam Generator Internal Loading Following a Main Steam or Feedwater Line Break," SMSAB-02-05, Office of Nuclear Regulatory Research, September, 2002.

5. S. Majumdar, S. Bakhtiari, K. Kasza, and J. Y. Park, "Validation of Failure and Leak Rate Correlations for Stress Corrosion Cracks in Steam Generator Tubes," NUREG/CR-6774, ANL-01/34, Argonne National Laboratory, May 2002.

6. A. Zahoor, "Ductile Fracture Handbook," Electric Power Research Institute, Palo Alto, CA, 1989.

7. L. A. James and D. P. Jones, "Fatigue Crack Growth Correlation for Austenitic Stainless Steels in Air", Proc. Conf. on Predictive Capabilities in Environmentally Assisted Cracking, R. Rungta, ed., PVP Vol. 99, American Society of Mechanical Engineers, NY, pp.363-414, 1985.

Appendix A Tests and Analysis of Failure of Degraded Tubes Under Internal Pressure and Bending Loading

A1 Introduction

Flexing of the tube support plates (TSPs) of a Model 51 steam generator (SG) during main-steam-line-break (MSLB) accidents transmits both axial and bending loads to the steam generator tubes (SGTs) that are locked at the carbon steel TSPs. The elastic finite element analyses that were conducted to assess the stresses in the SGTs due to such loads and to evaluate the stability of cracks in the SGTs due to such stresses ignored the effect of bending stresses on tube rupture (see Section 4.2.1). We carried out unit pressure load analyses in which each TSP was subjected to a unit pressure drop successively and the direct axial and bending stresses in a locked SGT were determined at all elevations above the tubesheet (TS) (Fig. 12b). To determine the net axial and bending stresses at all elevations, the unit pressure drop analysis results were used with the pressure drop information obtained from TH analyses across all of the TSPs.[4] It is evident from these results that the maximum bending stresses in the tube are small (≤10%) when compared with the maximum direct axial stresses. Therefore, in the evaluation of the stability of axial and circumferential cracks, the bending stresses were neglected (Section 4.2.1). The objective of the current series of tests and analyses is to show that neglecting the bending stresses in the determination of crack instability loads is justified and that the effect of the bending loads on the leakage from flawed tubes that remain stable is also small.

A2 Test Setup

The setups for the tests on MA Alloy 600 specimens [7/8-in. (22-mm) OD, 0.05-in. (1.3-mm) wall thickness] with axial and circumferential notches are shown schematically in Figs. A-1a and b, respectively. A 36-in.(91-cm)-long SG tube that contained an axial or circumferential EDM notch is clamped at one end (to simulate the tubesheet) and supported laterally at the other end (to simulate the first TSP). The nearest tip of the axial notch (1 in. long [25 mm]) is placed 2 in. (51 mm) away from the clamped end to minimize the effect of constraint on burst pressure. The results for this configuration should be conservative when compared with more realistic geometries with cracks closer to the TS. The circumferential notch is placed close to the clamped end so it is subjected to the maximum possible bending stress. The tube is first subjected to a fixed transverse bending load at the midspan and then pressurized at the rate of 2 ksi/s at room temperature in a high-pressure test facility until unstable rupture occurs. The specimens with PTW axial flaws were tested in 2 stages. In Stage 1 of the test procedure, they were pressurized until ligament rupture occurred. In Stage 2, an elastomer bladder and metal foil were inserted into the specimens, which were then pressurized at ≈2 ksi/s until unstable burst.

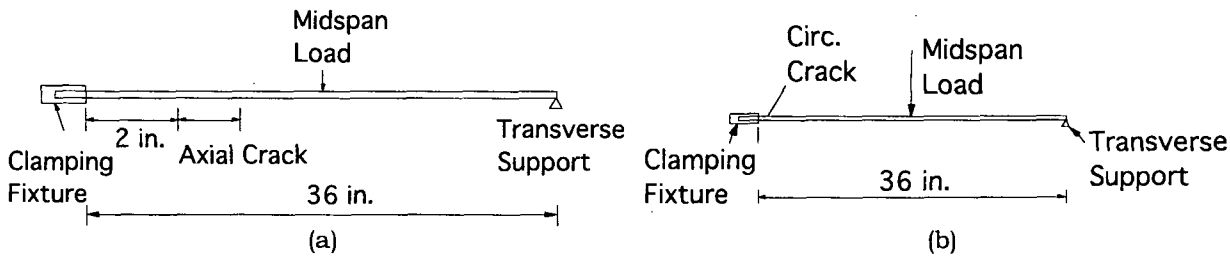

Figure A-1.Test setup for tubes with (a) axial and (b) circumferential cracks. Note 1 in. = 25.4 mm.

To provide a capability for transverse loading, the High-Pressure Test Facility containment module at ANL was modified. The 2-point fixture system for holding tubes, which had been used previously for burst/leak tests on shorter specimens, was modified by moving the 2 tube-end vertical supports to the ends of the 1/2-in. (13-mm) aluminum bed plate, yielding a 36-in. (91-cm) span between supports. One end support is used, with its 2-bolt clamp bar holding the tube rigid (this end represents the support of the tube sheet in the steam generator). The size of the hole in the second existing end support was increased slightly so that, when the 2-bolt clamp bar is in place, the tube can move axially but is constrained to only a small amount of movement transverse to the tube axis (which simulates a TSP). The overall length of the tube test specimens with a high-pressure water feed end fitting and the high-pressure valve for purging air from the specimens, exceeded the inside dimension of the containment and hence required that the access holes in the plastic end plates of the containment module be enlarged.

Dead weights were used to load the tubes transversely. The loading is applied by a multi-strand noose wire that slips over the tube at midspan and hangs downward off the bottom of the horizontal tube. Holes were drilled directly below the noose location through the bottom of the containment pipe and the 3 plates on the support cart. A loading plate that can be stacked with lead weights totaling from 0 to 200 lbs was attached to the wire.

A3 Background Analyses and Development of the Test Matrix

A.3.1 Axial Crack

Finite element analyses (FEAs) were conducted for the throughwall (TW) axial-crack geometries shown in Fig. A-1a. Cracks located both on the tensile bending side and on the compressive bending side of the tube were considered. A transverse load of 100 lbs was used. Figure A-2 shows the true stress-strain curve used in the FEA. Plots of the crack opening displacement (COD) profile as a function of pressure are shown in Figs. A-3a and b for cases where the crack is on the compressive bending side and the tensile bending side, respectively. When the crack is on the compressive side, the COD is slightly larger than when it is on the tensile side. Therefore, the burst pressure should be slightly lower when the crack is on the compressive side than when it is on the tensile side, but the difference is not expected to be large.

A.3.2 Circumferential Crack

A series of FEAs was also conducted for the TW circumferential crack geometries shown in Fig. A-1b, In this case, the crack is on the tensile bending side of the tube. Analyses were conducted for 240, 270, and 300° TW circumferential flaws. The maximum CODs as a function of pressure are shown in Figs. A-4-6 for 240, 270, and 300° circumferential TW cracks, respectively. The predicted unstable burst pressures for these cracks as functions of the applied transverse load are plotted in Fig. A-7 as solid lines. A typical calculated displaced-shape plot for a 300° crack with a 200-lb load at close to burst pressure is shown in Fig. A-8.

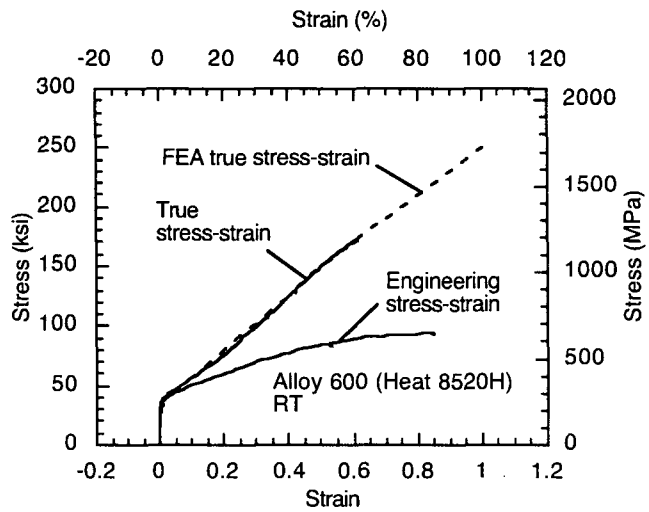

Figure A-2.
True stress-strain curve of Alloy 600 used in FEA.

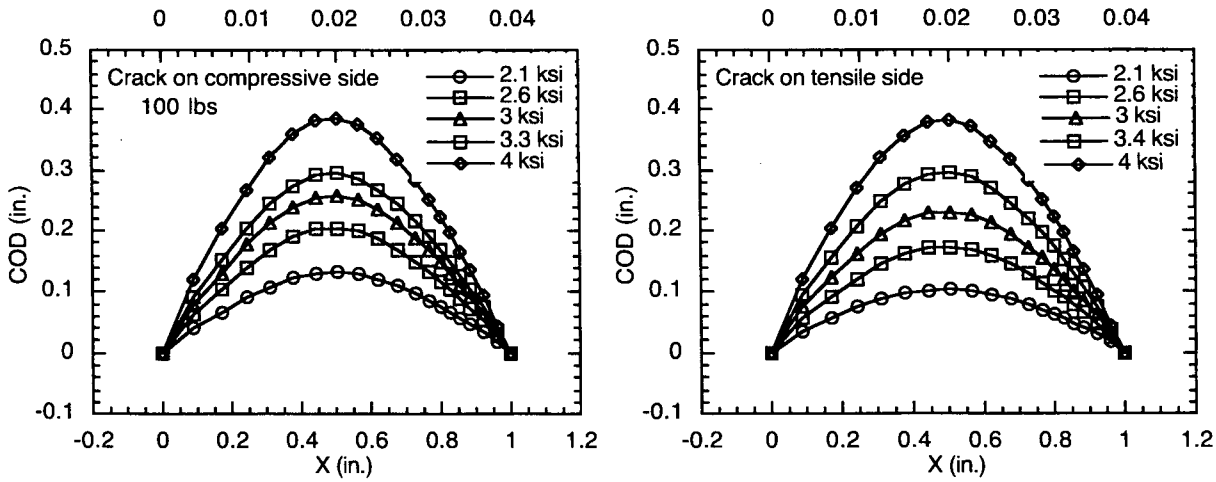

(a) (b)

Figure A-3.Calculated crack opening displacement (COD) profiles of 1 in. (25-mm)-long axial cracks under various pressures.

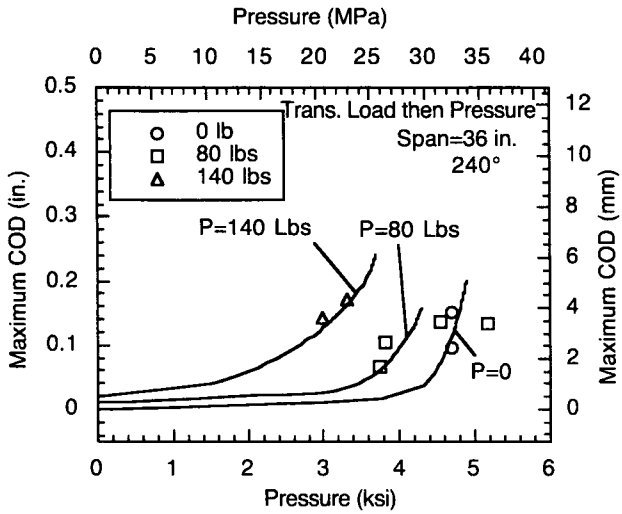

Figure A-4.
Maximum COD vs. pressure plot for 240° circumferential cracks. Symbols represent experimental results.

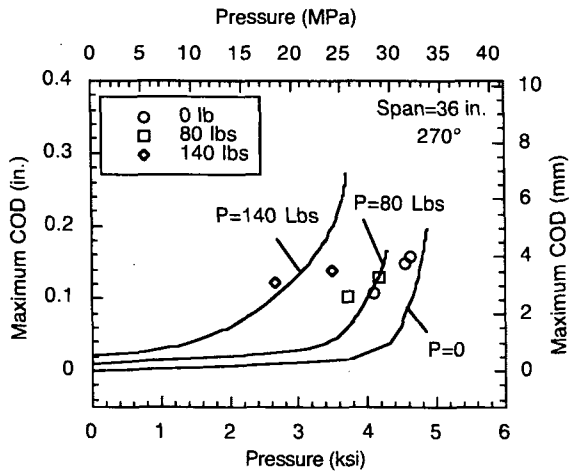

Figure A-5.
Maximum COD vs. pressure plot for 270° circumferential cracks. Symbols represent experimental results.

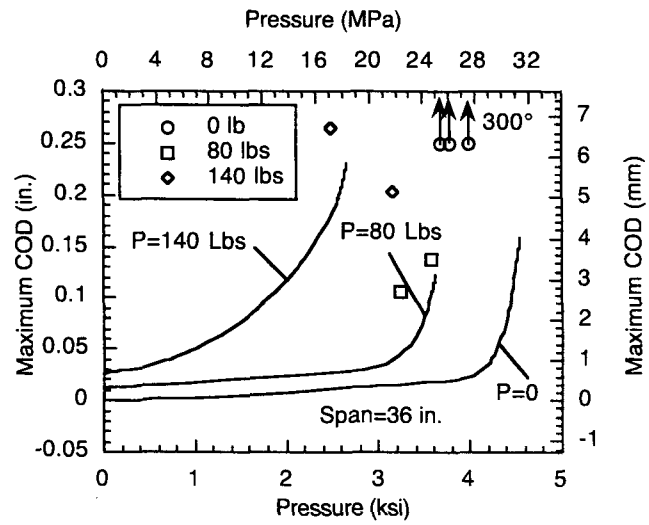

Figure A-6.
Maximum COD vs. pressure plot for 300° circumferential cracks. Symbols represent experimental results. Up arrows indicate specimens that burst and broke into 2 pieces.

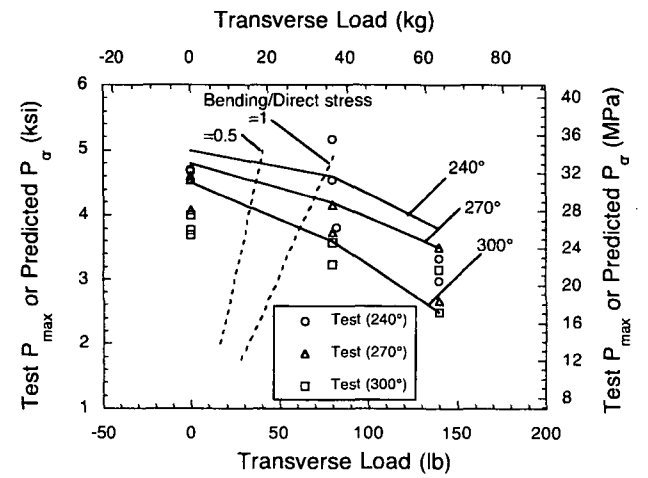

Figure A-7.
Variation of predicted burst pressure (solid lines) and test maximum pressures (symbols) with transverse load.

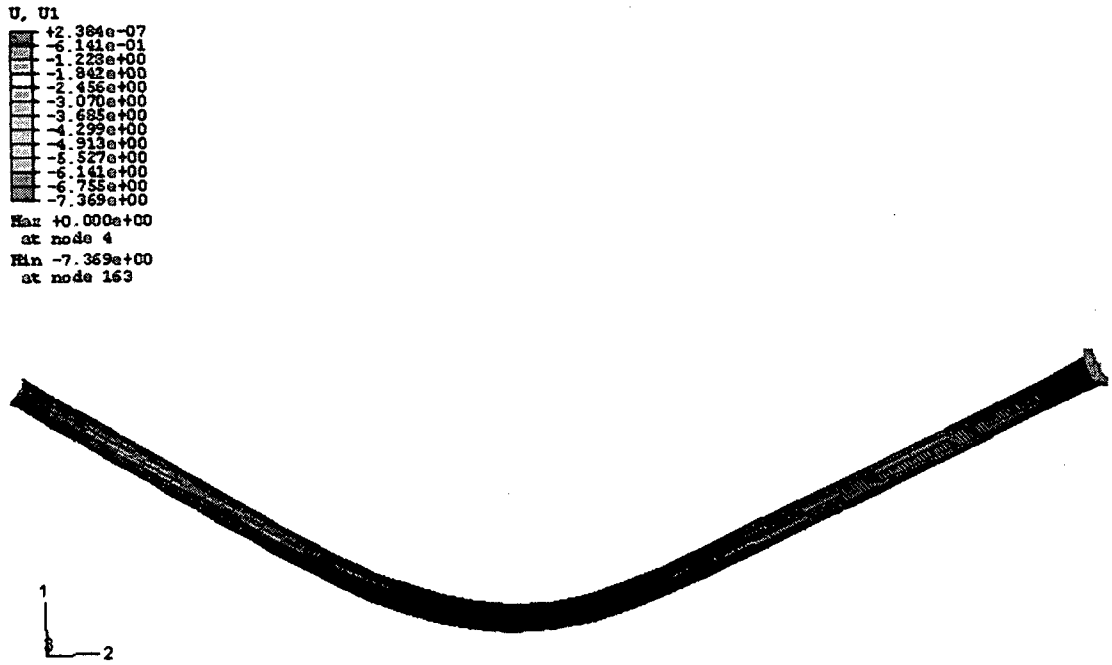

Figure A-8.Calculated displaced shape of 36-in. (91-cm)-long specimen with 300° circumferential crack at top of tubesheet with transverse load at midspan.

Note that the differences in the predicted failure pressures for the 3 cracks are not large. To have the possibility to burst the specimens unstably at the pressures within the capability of the high-pressure test facility, specimens with TW 240, 270, and 300° circumferential notches were selected. Based on the analyses presented above, 0, 80, and 140 lbs were selected as the transverse loads for the tests with circumferential flaws.

A4 Test Results

A summary of all of the tests with axial notchess is given in Table A-1 and those with circumferential notches, in Table A-2.

Table A-1. Flawed tube rupture tests of transversely loaded tubes with axial notches.

Tube ID and Test Date	Notch Type, Depth (% TW or radial extent), and Length	Load, kg (lb) and Test Conditions[a]	Tube Deflection, cm (in.):[b] preload loaded pretest loaded post-test/ unloaded post-test	Flaw Opening Pressure, M Pa (psi)	Fail. Mode[c]
5522-1 5/21/03	Axial, 80%, 25 mm (1 in.)	45 (100) T QS	Not measured.	22.1 (3200)	LT
5522-1 6/10/03	Axial, 100%; 25 mm (1-in.)	45 (100) T RR	17.94 (7.06) 17.38 (6.84) 17.46 (6.88) 17.94 (7.06)	12.8 (1863)	B
5507-2 5/28/03	Axial, 80%, 25 mm (1 in.)	45 (100) T QS	17.86 (7.03) 17.46 (6.88) 17.46 (6.88) 17.86 (7.03)	21.5 (3125)	LT
5507-2 6/9/03	Axial, 100%; 25 mm (1-in.)	45 (100) T RR	17.78 (7.00) 17.46 (6.88) 17.38 (6.84) 17.94 (7.06)	14.9 (2167)	B
8520-3A 6/10/03	Axial, 100%; 25 mm (1-in.)	45 (100) B RR	17.86 (7.03) 17.30 (6.81) 17.30 (6.81) 17.82 (7.02)	14.8 (2145)	B
8520-3B 6/11/03	Axial, 80%, 25 mm (1 in.)	0 (0) T QS	17.62 (6.94) 17.62 (6.94) 17.62 (6.94) 17.62 (6.94)	17.3 (2510)	LT
8520-3B 6/19/03	Axial, 100%; 25 mm (1-in.)	0 (0) T QS	18.18 (7.16)	14.4 (2093)	B

Table A-1 Flawed tube rupture tests of transversely loaded tubes with axial notches (cont'd)

Tube ID and Test Date	Notch Type, Depth (% TW or radial extent), and Length	Load, kg (lb) and Test Conditions[a]	Tube Deflection, cm (in.)[b]: preload/ loaded pretest/ loaded post-test/ unloaded post-test	Flaw Opening Pressure, M Pa (psi)	Fail. Mode[c]
8520-4 6/11/03	Axial, 80%, 25 mm (1 in.)	64 (140) T QS	17.15 (6.75) 16.67 (6.56) 16.67 (6.56) 17.30 (6.81)	25.7 (3734)	LT
8520-4 6/20/03	Axial, 100%, 25 mm (1 in.)	64 (140) T RR	-	15.8 (2298)	B
8520-5 6/20/03	Axial, 100%, 25 mm (1 in.)	64 (140) B RR	-	14.1 (2038)	B
8520-6 6/12/03	Axial, 80%, 25 mm (1 in.)	0 (0) T QS	17.46 (6.88)	19.1 (2770)	LT
8520-6 6/20/03	Axial, 100%, 25 mm (1 in.)	0 (0) T RR	-	15.9 (2303)	B
8520-7 6/13/03	Axial, 80%, 25 mm (1 in.)	64 (140) T QS	17.70 (6.97) 16.99 (6.69) 16.67 (6.56) 17.30 (6.81)	20.3 (2940)	LT
8520-7 6/19/03	Axial, 100%, 25 mm (1 in.)	64 (140) T RR	17.94 (7.06) 17.15 (6.75) 16.99 (6.69) 17.70 (6.97)	14.3 (2078)	B

[a] T = flaw on top during test; B = flaw on bottom during test; QS = quasi-steady pressure ramp rate; RR = 13.8 MPa/s (2000 psi/s) ramp rate during test.

[b] Tube deflection is measured as distance from top of tube to underlying base plate. Thus, a smaller value indicates a larger deflection.

[c] LT = ligament tearing; B = unstable burst; No = no failure.

Table A-2. Flawed tube rupture tests of transversely loaded tubes with circumferential notches

Tube ID and Test Date	Notch Type, Depth (% TW or radial extent), and Length	Load, kg (lb) and Test Conditions[a]	Tube Deflection, cm (in.):[b] preload loaded pretest loaded post-test unloaded post-test	Flaw Opening Pressure, M Pa (psi)	Fail. Mode[c]	Max. Flaw Opening mm (in.)
5526-4 5/30/03	Circ., 90%; 240°	36 (80) T QS	17.94 (7.06) 17.62 (6.94) 17.46 (6.88) 17.94 (7.06)	5.10 (740)	LT	
5526-4 6/9/03	Circ. 100%, 240°	36 (80) T RR	17.94 (7.06) 17.46 (6.88) 15.56 (6.12) 17.46 (6.31)	35.6 (5160)	B	3.4 (0.134)
8520-12 6/10/03	Circ. 100% 240°	36 (80) T RR	17.94 (7.06) 17.38 (6.84) 15.80 (6.22) 16.35 (6.44)	31.3 (4543)	B	3.51 (0.138)
8520-14 6/10/03	Circ. 100% 240°	0 (0) T RR	18.57 (7.31) 18.57 (7.31) 17.94 (7.06) 17.94 (7.06)	32.3 (4688)	B	2.41 (0.095)
8520-15 6/11/03	Circ. 100% 240°	0 (0) T RR	Not measured	32.5 (4704)	No	3.89 (0.153)
8520-16 6/12/03	Circ. 100% 240°	63 (140) T RR	18.1 (7.13) 16.75 (6.59) 11.43 (4.5) 12.54 (4.94)	20.6 (2982)	No	3.66 (0.144)
8520-17 6/17/03	Circ. 100% 240°	36 (80) T RR	17.94 (7.06) 17.46 (6.88) 15.00 (5.91) 15.56 (6.13)	25.8 (3743)	No	1.74 (0.0685)
8520-18 6/17/03	Circ. 100% 240°	63 (140) T RR	15.88 (6.25) 14.92 (5.88) 10.16 (4.00) 11.11 (4.38)	22.9 (3318)	No	4.37 (0.172)
8520-19 6/11/03	Circ. 100% 270°	0 (0) T RR	17.38 (6.84) 17.38 (6.84) 17.38 (6.84) 17.07 (6.72)	31.8 (4615)	No	4.04 (0.159)

Table A-2 Flawed tube rupture tests of transversely loaded tubes with circumferential notches (cont'd)

Tube ID and Test Date	Notch Type, Depth (% TW or radial extent), and Length	Load, kg (lb) and Test Conditions[a]	Tube Deflection, cm (in.)[b]: preload/ loaded pretest/ loaded post-test/ unloaded post-test	Flaw Opening Pressure, M Pa (psi)	Fail. Mode[c]	Max. Flaw Opening mm (in.)
8520-26 6/12/03	Circ. 100% 300°	0 (0) T RR	17.86 (7.03)	26.0 (3777)	B	Broke in 2 pieces
8520-25 6/17/03	Circ. 100% 270°	64 (140) T RR	16.19 (6.38) 12.94 (5.09) 11.59 (4.56) 12.70 (5.00)	18.4 (2665)	No	3.11 (0.1225)
8520-27 6/13/03	Circ. 100% 300°	0 (0) T RR	17.70 (6.97)	25.4 (3691)	B	Broke in 2 pieces
8520-1x 6/13/03	Circ. 100% 300°	36 (80) T RR	17.15 (6.75) 16.35 (6.44) 15.56 (6.13) 16.11 (6.34)	24.7 (3580)	No	3.51 (0.138)
8520-2x 6/13/03	Circ. 100% 300°	64 (140) T RR	16.27 (6.41) 15.08 (5.94 10.64 (4.19) 11.51 (4.53)	21.8 (3157)	No	5.18 (0.204)
8520-3x 6/17/03	Circ. 100% 300°	36 (80) T RR	17.94 (7.06) 17.38 (6.84) 15.56 (6.13) 16.19 (6.38)	22.3 (3235)	No	2.72 (0.107)
8520-4x 6/18/03	Circ. 100% 300°	64 (140) T RR	16.43 (6.47) 15.08 (5.94) 10.24 (4.03) 11.27 (4.44)	17.2 (2493)	No	6.73 (0.265)

Table A-2 Flawed tube rupture tests of transversely loaded tubes with circumferential notches (cont'd)

Tube ID and Test Date	Notch Type, Depth (% TW or radial extent), and Length	Load, kg (lb) and Test Conditions[a]	Tube Deflection, cm (in.)[b]: preload/ loaded pretest/ loaded post-test/ unloaded post-test	Flaw Opening Pressure, M Pa (psi)	Fail. Mode[c]	Max. Flaw Opening mm (in.)
8520-5x 6/30/03	Circ; 100%; 240°	36 (80) T RR	17.30 (6.81) 16.75 (6.59) 14.92 (5.88) 15.48 (6.09)	26.3 (3820)	No	2.68 (0.106)
8520-6x 6/30/03	Circ; 100%; 270°	0 (0) T RR	17.30 (6.81) 17.30 (6.81) 17.07 (6.72) 17.07 (6.72)	28.2 (4089)	No	2.73 (0.108)
8520-7x 6/30/03	Circ; 100%; 300°	0 (0) T RR	17.30 (6.81) 17.30 (6.81) 16.99 (6.69 16.99 (6.69	27.6 (4001)	B	Broke in 2 pieces

[a] T = flaw on top during test; B = flaw on bottom during test; QS = quasi-steady pressure ramp rate; RR = 13.8 MPa/s (2000 psi/s) ramp rate during test.

[b] Tube deflection is measured as distance from top of tube to underlying base plate. Thus, a smaller value indicates a larger deflection.

[c] LT = ligament tearing; B = unstable burst; No = no failure.

A.4.1 Axial Notches

The tests were conducted with zero, 100-, and 140-lb transverse loads, with the notches located either on the tensile side (top) or on the compressive side (bottom) of the specimens. The typical appearance of axial notches after ligament rupture and after unstable burst is shown in Figs 9a and b. The test results are summarized in Table A-1 and Fig. A-10. None of the specimens displayed significant bending after ligament rupture or unstable burst. For all of the specimens, the ligament rupture pressures (Stage 1) increased with increasing transverse load. As expected, the ligament rupture pressures of the specimens with the axial notches on the tensile side (top) were slightly higher than those of specimens with notches on the compressive side (bottom). The specimens that were subsequently pressurized until unstable burst (stage 2 testing with bladder and foil) displayed burst pressures that were lower than the ligament rupture pressures, indicating that they would have burst unstably during stage 1 of the testing if the flow capacity of the pump was adequate. Unlike the ligament rupture pressures of the 80% part-throughwall notches, the unstable burst pressures of the 100% TW notches are relatively insensitive to the applied transverse load, in agreement with the FEA results. The dashed lines in Fig. A-10 show the loading

combinations for which the bending-to-axial-direct-stress ratios are 0.5 and 1. Because the maximum expected stress ratio during MSLB is of the order of 0.1 (Fig. A-1b), the effects of the bending stresses on both the ligament rupture and the unstable burst pressures will be very small.

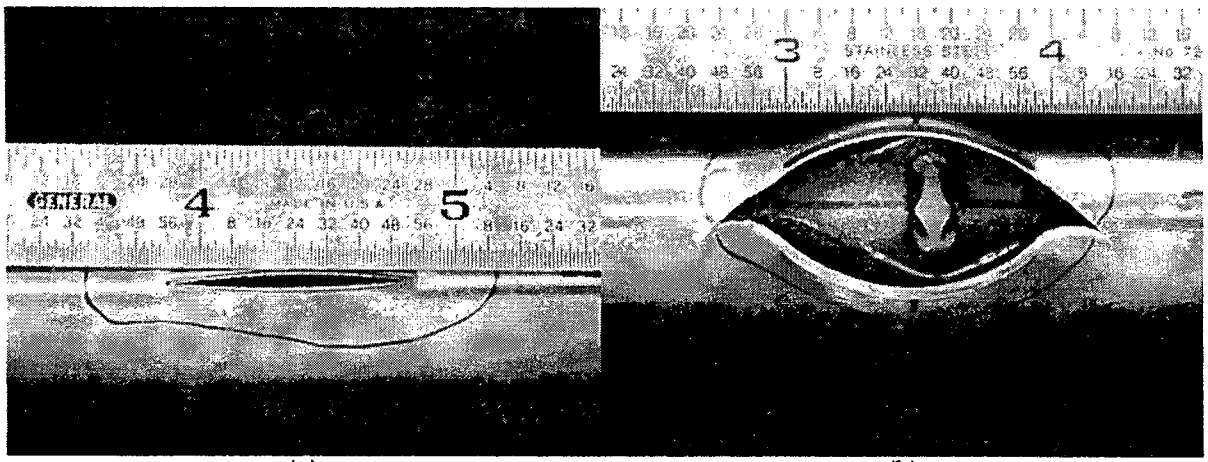

(a) (b)

Figure A-9.Typical view of specimen with axial notch (a) after ligament rupture (Stage 1) and (b) after unstable burst (Stage 2).

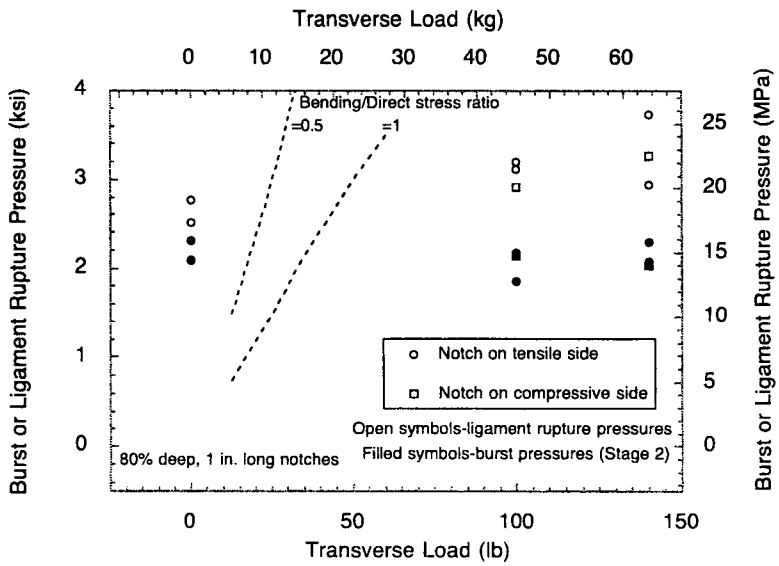

Figure A-10.
Variation of ligament rupture and burst pressures with applied transverse load for specimens with axial notches.

A.4.2 Circumferential Notches

Tests were conducted with zero, 80-, and 140-lb transverse loads with notches located on the tensile side (top) of the specimens. The test results are summarized in Table A-2. All specimens showed significant bending displacement during and after the tests (Fig. A-11). Except for 2 cases with 300° notches, the specimens did not burst or break into 2 pieces. Typically, the tests were stopped when the bladder and foil ruptured and the specimens could

not be pressurized any further. Therefore, the maximum pressures attained during the tests represent bounds that were lower than those of unstable burst pressures. However, in almost all cases, the CODs of the notches at the end of the tests were significant (≥ 0.1 in.)(Table A-2). The measured CODs and the maximum pressures attained in the tests are shown as symbols in Figs. A-4-6. In all cases except the 300° notch at zero transverse load, the predicted CODs are reasonably close to the observed CODs. Because the calculated COD-vs.-pressure curves show a rapidly increasing slope at the final notch opening, the true burst pressures of the specimens are very likely close to the experimentally attained maximum pressures. Thus, the predicted unstable burst pressures (defined as pressures when the COD = 0.25 in.) are reasonably close to the experimentally observed maximum pressures (Fig. A-7), except for the 300° notches with zero transverse load. The dashed lines in Fig. A-7 show the loading combinations for which the bending-to-axial-direct-stress ratios are 0.5 and 1. Inasmuch as the maximum expected stress ratio during a MSLB is of the order of 0.1 (Fig. A-12), the bending stresses will exert an insignificant effect on the unstable burst pressures.

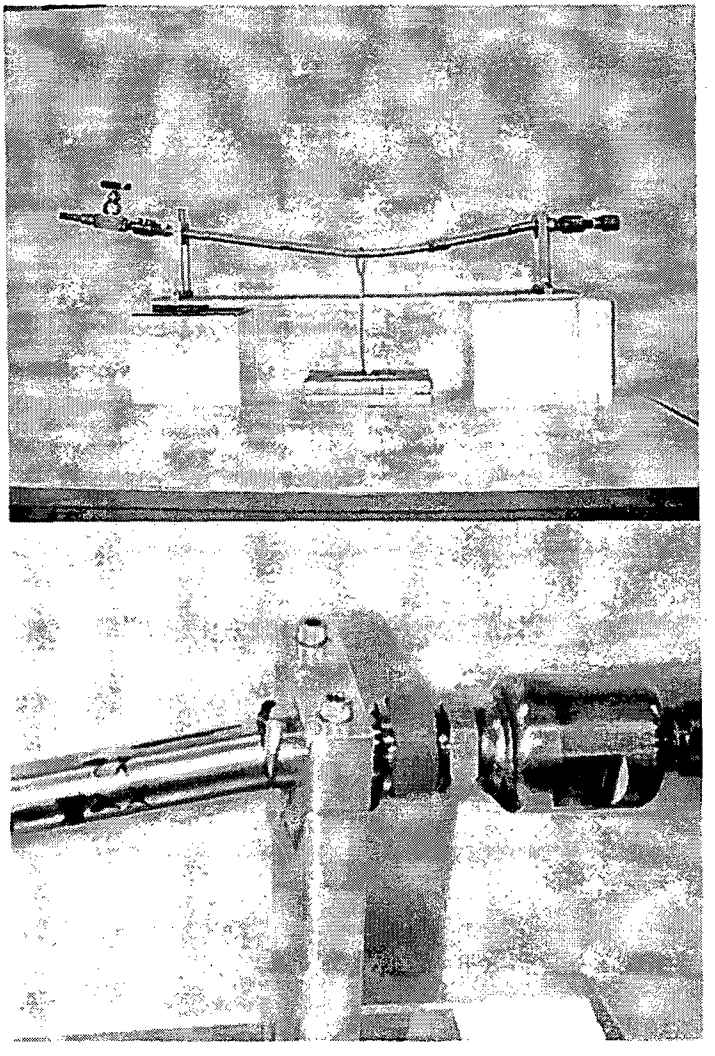

Figure A-11. Post-test view of specimen with circumferential flaw and closeup view of end of tube with the notch.

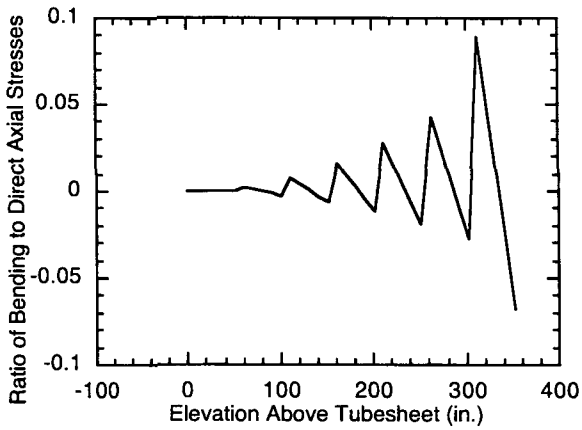

Figure A-12.
Variation of ratio of bending-to-direct-axial-stresses during MSLB

The burst pressure of specimens with a TW circumferential crack can be calculated by using a net-section-collapse model in which the axial load due to the internal pressure is assumed to cause collapse of the net uncracked section of the tube. These burst pressures are significantly higher than those in the case in which the tube is free to bend (zero constraint). In earlier work we have shown that the degree of constraint to bending is determined by the nondimensional parameter c, defined as

$$c = \frac{\pi E \delta_c}{4 L_e \bar{\sigma}} \tag{4}$$

where E =Young's modulus, L_e = effective length of the tube (= L/3 for fixed-pinned beams), $\bar{\sigma}$ = flow stress, and δ_c = critical crack tip opening displacement (CTOD). For the free-to-bend condition, c = 0 and, for the fully constrained condition, c = ∞. In our case, substituting E = 28,000 ksi, L_e = 36/3 = 12 in., $\bar{\sigma}$ = 78.5 ksi, and critical CTOD δ_c = 0.05 in. (corresponds to $K_{JC} \approx$ 350 ksi-√in), c = 1.2. A plot of the predicted burst pressures normalized by the unflawed burst pressure (9.5 ksi), shown in Fig. 13, suggests that, for c = 1.2, cracks ≥240° should behave as fully constrained.

Figure A-13 shows the predicted and observed maximum test pressures for specimens tested without applied transverse loads. The predicted burst pressures are close to the observed burst pressures for the specimens with 300° notches. For the specimens with shorter notches, which did not burst, the maximum test pressures do lie below the predicted burst pressure line.

To explore the effect of bending load on the leakage rate through circumferential cracks during a MSLB accident, the crack opening area at a pressure differential of 2.5 ksi is plotted as a function of the transverse load and crack angle in Fig. A-14. Although the crack opening area at large bending-to-axial direct stress ratios (> 2) can be large when compared with that at zero bending load, the effects on the crack opening area at the expected bending to axial stress ratio of ≈0.1 during a MSLB is very small.

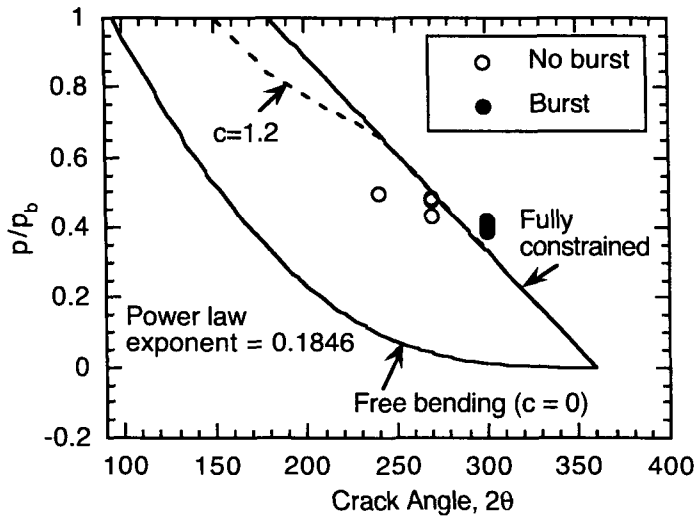

Figure A-13.
Observed test pressures vs. burst pressures predicted by net section collapse (fully constrained, c = ∞), free bending (c = 0), and ANL model with c = 1.2 for specimens with no applied transverse load.

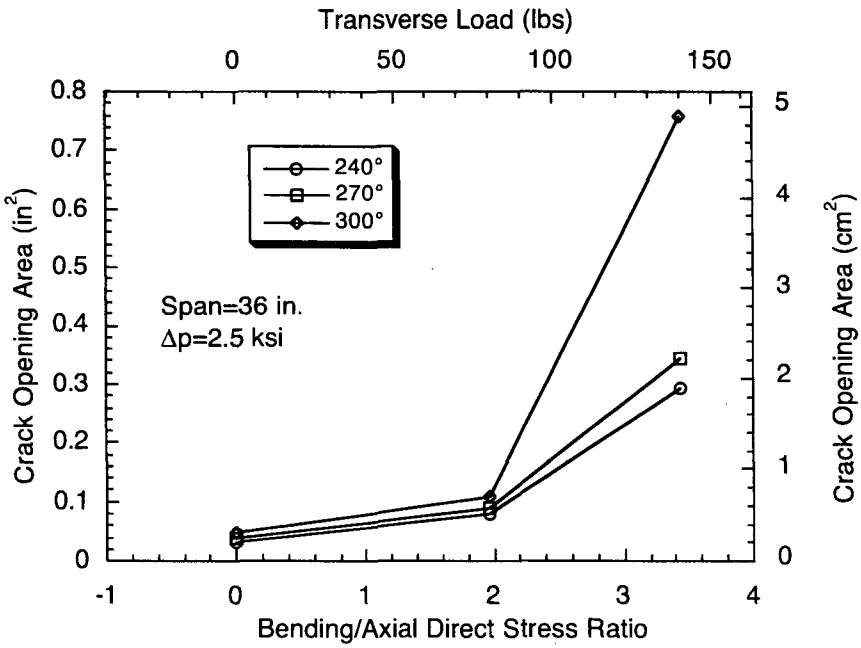

Figure A-14.
Effect of transverse load on circumferential crack opening area.

A5 Conclusions

Burst tests were conducted on 36-in. (91-cm)-long Alloy 600 tubes with 1-in. (25-mm)-long axial and 240, 270 and 300° circumferential EDM notches at the clamped end, simply supported at the other end, and with various transverse loads hung at the midspan. The results showed that the effect of the transverse load on burst pressure was much more pronounced on the specimens with a circumferential notch than on those with axial notch. For the PTW axial notch, the ligament rupture pressure increased slightly with increasing transverse load. The burst pressure of the TW axial notch was relatively insensitive to the transverse load.

For specimens with a TW circumferential notch, the maximum notch opening displacement increased and the burst pressure decreased with increasing transverse load. However, for the expected bending-to-direct-axial-stress during an MSLB accident, the reduction in burst pressure is negligible.

The test results were consistent with finite-element predictions.

NRC FORM 335
(9-2004)
NRCMD 3.7

U. S. NUCLEAR REGULATORY COMMISSION

BIBLIOGRAPHIC DATA SHEET

(See instructions on the reverse)

1. REPORT NUMBER
(Assigned by NRC. Add Vol., Supp., Rev., and Addendum Numbers, if any.)

NUREG/CR-6935

2. TITLE AND SUBTITLE

Sensitivity Studies of Failure of Steam Generator Tubes during Main Steam Line Break and Other Secondary Side Depressurization Events

3. DATE REPORT PUBLISHED

MONTH	YEAR
May	2007

4. FIN OR GRANT NUMBER

Y6588

5. AUTHOR(S)

Saurin Majumdar, Ken Kasza, John Oras, Jeff Franklin, and Charles Vulyak, Jr.

6. TYPE OF REPORT

7. PERIOD COVERED (Inclusive Dates)

8. PERFORMING ORGANIZATION – NAME AND ADDRESS *(If NRC, provide Division, Office or Region, U.S. Nuclear Regulatory Commission, and mailing address; if contractor, provide name and mailing address.)*

Argonne National Laboratory
9700 South Cass Avenue
Argonne, IL 60439

9. SPONSORING ORGANIZATION – NAME AND ADDRESS *(If NRC, type "Same as above": if contractor, provide NRC Division, Office or Region, U.S. Nuclear Regulatory Commission, and mailing address.)*

Division of Fuel, Engineering and Radiological Research
Office of Nuclear Regulatory Research
U.S. Nuclear Regulatory Commission
Washington, DC 20555–0001

10. SUPPLEMENTARY NOTES

Eric Reichelt, NRC Project Manager

11. ABSTRACT (200 words or less)

This report summarizes sensitivity studies conducted on the failure of flawed steam generator tubes in a Westinghouse Model 51 steam generator (SG) during main steam line break (MSLB) and feed water line break (FWLB) events. The results of thermal hydraulic transient analysis of temperature and pressure pulse loading during the MSLB and FWLB events were obtained from a recent Nuclear Regulatory Commission (NRC) report. A simplified but conservative finite element model of the tube support plates (TSPs) and their supports and SG tubes was used to analyze the loads transferred to the SG tubes from the TSPs during the transients. Fracture mechanics analyses were conducted to determine the stability of postulated cracks in the SG tubes on the top of the tube sheet and the TSPs. The potential for crack growth during repeated application of the pressure pulse was explored. Tests on SG tubes subjected to bending load and internal pressure showed that the effect of bending on burst pressure is negligible for the type of bending-to-direct-axial-stress ratio that is expected during a MSLB.

12. KEY WORDS/DESCRIPTORS *(List words or phrases that will assist researchers in*

Steam Generator Tube Integrity
Tube Support Plate
Main Steam Line Break
Feed Water Line Break
Axial Cracks
Circumferential Cracks
Tube Burst
Bending Effect on Burst Pressure

13. AVAILABILITY STATEMENT
unlimited

14. SECURITY CLASSIFICATION
(This Page)
unclassified
(This Report)
unclassified

15. NUMBER OF PAGES

16.PRICE

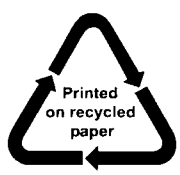

Federal Recycling Program

UNITED STATES
NUCLEAR REGULATORY COMMISSION
WASHINGTON, DC 20555-0001

OFFICIAL BUSINESS